

Elongated Titanate Nanostructures and Their Applications

Dmitry V. Bavykin*^[a] and Frank C. Walsh^[a]

Keywords: Layered compounds / Nanostructures / Titanium dioxide / Titanates

Recent advances in the synthesis, characterisation and applications of elongated titanate and TiO₂ nanostructures (including nanotubes, nanofibres and nanorods) are reviewed. The physicochemical properties of nanostructures, such as high surface area, efficient ion-exchange properties, electron and proton conductivity and high aspect ratio, are described in connection with a particular application. Practical aspects of the preparation, stability and transformation of elongated titanates are considered. A critical survey of the literature is

provided together with the development of prospective energy applications of elongated titanates in catalysis, photocatalysis, electrocatalysis, solar cells, fuel cells, lithium batteries and hydrogen storage. Other applications utilising the high aspect ratio of elongated nanostructures include biomedical implants, sensors, drug delivery systems and smart, tribological composite coatings.

(© Wiley-VCH Verlag GmbH & Co. KGaA, 69451 Weinheim, Germany, 2009)

Contents:

1. Introduction
2. Advances in the Synthesis of Elongated Titanates
 - 2.1. Synthesis
 - 2.2. Structure
 - 2.3. Mechanism of Titanate Nanotube Formation
 - 2.3.1. Stability and Transformations of Elongated Titanates
3. Applications
 - 3.1. Reaction Catalysis
 - 3.2. Electrocatalytic Storage or Generation of Electricity

- 3.2.1. Fuel Cells and Batteries
- 3.2.2. Lithium Batteries
- 3.2.3. Supercapacitors and General Electrochemistry
- 3.3. Photocatalysis in Elongated Titanates
- 3.4. Solar Cells
- 3.5. New Materials
 - 3.5.1. Magnetic Materials
 - 3.5.2. Hydrogen Storage and Sensing
 - 3.5.3. Composites, Surface Coatings and Tribology
- 3.6. Biomedical Applications
- 3.7. Other Applications
4. Conclusions

[a] Electrochemical Engineering Laboratory, Materials Engineering and Energy Technology Research Groups, School of Engineering Sciences, University of Southampton, Highfield, Southampton SO17 1BJ, United Kingdom



Dr. Dmitry Bavykin received an MSc (Chemistry) at Novosibirsk State University in 1995 and a PhD (Chemical Engineering) at Borekov's Institute of Catalysis, Novosibirsk in 1998. He was awarded a NATO/Royal Society Fellowship in 2002 to study the preparation, characterisation and application of titanium dioxide nanotubes in electrochemistry and catalysis at the University of Bath. Currently, he is a Lecturer in Energy Technology Research Group in the School of Engineering Sciences at the University of Southampton. His major area of interest is the application of novel, nanostructured materials to renewable energy problems.



Frank Walsh is currently Director of the Research Institute for Industry, Professor in Electrochemical Engineering and Deputy Head (Enterprise) in the School of Engineering Sciences at the University of Southampton, UK. He directs the research activities of the Electrochemical Engineering Laboratory in the Energy Technology Research Group. His research output, which spans the areas of energy conversion, electroactive nanomaterials, coating technology, electrochemical monitoring and sensors, corrosion, surface finishing and electrochemical process engineering, includes four text books, 70 short course papers, more than 200 conference presentations, more than 260 research papers and more than 50 educational papers.

1. Introduction

Despite the relatively high abundance of titanium in nature and the low toxicity of most of its inorganic compounds, the metallurgical cost of extracting titanium metal is high because of the complexity of the traditional Kroll molten salt extraction process. The original demand from the aerospace and rocket jet industries for the light and high-melting-temperature metal in the late 1940s stimulated improvements in the Kroll extraction process and initiated large-scale titanium production. In the late 1960s, approximately 80% of the titanium produced was used by the aerospace industry and 20% by other industries.^[1] Further reductions in the manufacturing cost of titanium have also stimulated the use of titanium compounds. Titanium dioxide has long been used as a white pigment in paints and polymers. Following the discovery of photocatalytic water splitting with TiO₂ under UV light^[2] in the late 1970s, a new era of TiO₂-based materials has emerged.^[3]

Over the last two decades, improvements in technology have allowed synthesis and manipulation of materials of the nanometre scale, resulting in an exponential growth of research activities devoted to nanoscience and nanotechnology. It is now appreciated that the physicochemical properties of nanomaterials can be significantly different from those of bulk materials, which opens up opportunities for the development of materials with unusual or tailored properties. This has stimulated the search for methods of controlling the size, shape, crystal structure and surface properties of nanomaterials in order to tailor them for a particular application.

Similar trends have been observed during the synthesis of nanostructured titanium dioxide and titanate materials. Initially, many of the nanostructured TiO₂ materials, normally produced by a variety of sol-gel techniques, consisted of spheroidal particles whose size varied over a wide range down to a few nanometres. The most promising applications of such TiO₂ nanomaterials were photocatalysis, dye-sensitised photovoltaic cells and sensors.^[3]

In 1998, Kasuga et al.^[4] discovered the alkaline hydrothermal route for the synthesis of titanium oxide nanostructures having a tubular shape. The search for nanotubular materials was inspired by the discovery of carbon nanotubes in 1991.^[5] Studies of their elegant structure and unusual physicochemical behaviour have significantly improved our fundamental understanding of nanosized structures. In contrast to carbon nanostructures, titanate and titanium dioxide nanotubes are readily synthesised by using simple chemical (e.g. hydrothermal) methods as low-cost materials.

Following the discovery of titanate nanotubes, many efforts have been made to (a) understand the mechanism of nanotube formation, (b) improve the method of synthesis and (c) thoroughly study the properties of nanotubes. Other elongated morphologies of nanostructured titanates, including nanorods, nanofibres and nanosheets, have also been found. Many data have been collected in recent, critical reviews.^[6–9]

Under alkaline hydrothermal conditions, the formation of titanate nanotubes occurs spontaneously and is characterised by a wide distribution of morphological parameters together with a random orientation of nanotubes. An alternative method, which facilitates the production of structured arrays of nanotubes with a narrower distribution of morphological parameters, is anodising. Anodic synthesis was initially developed for the preparation of aluminium oxide nanotubes and later adapted for TiO₂ nanotubular arrays. The method includes anodic oxidation of titanium metal in an electrolyte usually containing fluoride ions. Control of the fabrication conditions enables variation of the internal diameter of such nanotubes from 20 to 250 nm, their wall thickness from 5 to 35 nm and their length up to hundreds of microns.^[10] Several major reviews, which consider the fabrication, properties and various applications of these ordered TiO₂ nanotubular coatings, have recently been published.^[10–12]

The third general method for the preparation of elongated TiO₂ nanostructures is template-assisted sol-gel synthesis. This technique is versatile (but can be expensive) and is reviewed elsewhere.^[13]

The pool of published work in the area of elongated titanates and TiO₂ can be classified according to several themes: (a) improvements in the method of nanostructure preparation towards a better control of morphology and a lowered cost of manufacture, which includes studies of mechanisms of their formation, (b) exploration of the physicochemical properties of novel nanostructures with a focus on potential applications and (c) attempts to use elongated titanates in a wide range of applications. Since the discovery of titanate nanotubes, the amount of published work related to the first two themes has rapidly grown (and may be approaching a steady state), whereas the third theme has appeared only recently and is experiencing rapid growth.

This review is, therefore, focused on the critical evaluation and comparison of recently emerged applications of titanate and titanium dioxide elongated nanostructures. The most probable applications are highlighted and gaps in our knowledge are recognised, identifying the directions for further key studies. Future advances in the field of elongated titanate nanostructures are critically considered.

2. Advances in the Synthesis of Elongated Titanates

The literature contains many nonsystematic references to different morphological forms of elongated titanate nanostructures, which can result in confusion. Figure 1 defines the typical morphological forms that will be referred to in this review, namely the nanosheet (NS), nanotube (NT), nanorod (NR), nanofibre (NF) and nanoparticle (NP). Nanosheets are planar, two-dimensional structures; nanotubes are cylindrical structures with a characteristic hollow cavity through the centre along their length; nanorods are solid cylindrical structures with a circular base; nanofibres

are long parallelepiped-shaped structures and nanoparticles are spheroidal in shape. Frequently used terms such as nanowires, nanobelts and nanoribbons can be generally classified as nanofibres. The abbreviations “TiNT” and “TiNF” are used in this paper to refer to titanate nanotubes and titanate nanofibres, respectively.

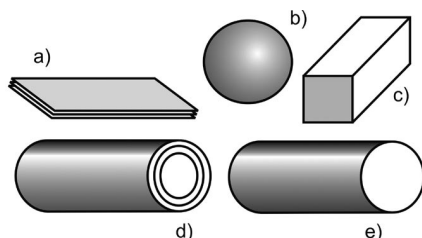


Figure 1. Typical morphologies of elongated titanate nanostructures: (a) sheets, (b) spheroids, (c) rectangular-section fibres, (d) multiple-wall nanotubes and (e) circular-section rods.

2.1. Synthesis

Since its introduction,^[4] many efforts have been made to develop the alkaline hydrothermal synthesis of titanate nanotubes towards a more suitable technological process allowing a facile and low-cost scale-up of the production. Potential routes for the preparation of titanate nanotubes are shown in Figure 2. The original method (route 1 in Figure 2) includes the use of TiO_2 raw material in aqueous 10 M NaOH at temperatures in the range 110–150 °C for 24 hours. The form of the TiO_2 reactant can include anatase, rutile, amorphous TiO_2 , or even Ti metal. The choice of initial raw material may affect the morphology of the resultant nanotubes, but no systematic data is available. The hydrothermal method traditionally requires the use of an autoclave with chemically resistant vessels [usually lined with poly(tetrafluoroethylene) (PTFE)], which can with-

stand such a concentrated and hot alkaline environment. On the other hand, the benefits of the method are a single process stage and relatively low hydrothermal temperatures to achieve an essentially complete conversion of initial raw materials to titanate nanotubes. Most of the recent modifications of the process have been targeted towards better control of the morphology (including the length, diameter and size of agglomerates) of nanotubes, reduction in the synthesis temperature and process intensification.

Effective ways to adjust the average length of the nanotubes include ultrasonic treatment of initial raw TiO_2 ^[14] or the improvement of mass transport conditions during alkaline hydrothermal treatment,^[15] which probably improves the dynamics of nanotube growth in the axial direction by making available dissolved titanium(IV) species. The average diameter of nanotubes can be controlled, to some extent, by the synthesis temperature.^[16] A degree of control over the shape of the nanotubular agglomerates can be achieved by using either hydrogen peroxide^[17] or a controlled initial particle size distribution for the raw TiO_2 .^[14]

There are several approaches to the intensification of the process of nanotubular titanate growth, including microwave heating^[18–21] or ultrasonication^[22] of the reaction mixture during synthesis, improvement of mixing by using a revolving autoclave^[23] or a hot press fabrication method.^[24] All of these approaches allow the synthesis time to be reduced from 24 h down to a few hours.

The need to use pressurised reactors for preparation of the nanotubes greatly increases the manufacturing cost and complicates health and safety requirements. Attempts to avoid autoclave operations by reduction of the synthesis temperature below the boiling temperature of the alkaline solution (ca. 106 °C) usually result in the formation of multilayered, lepidocrocite-type nanostructures (nanosheets) instead of nanotubes.^[25] There are several reports, however, of titanate nanotubes obtained under reflux conditions.^[26]

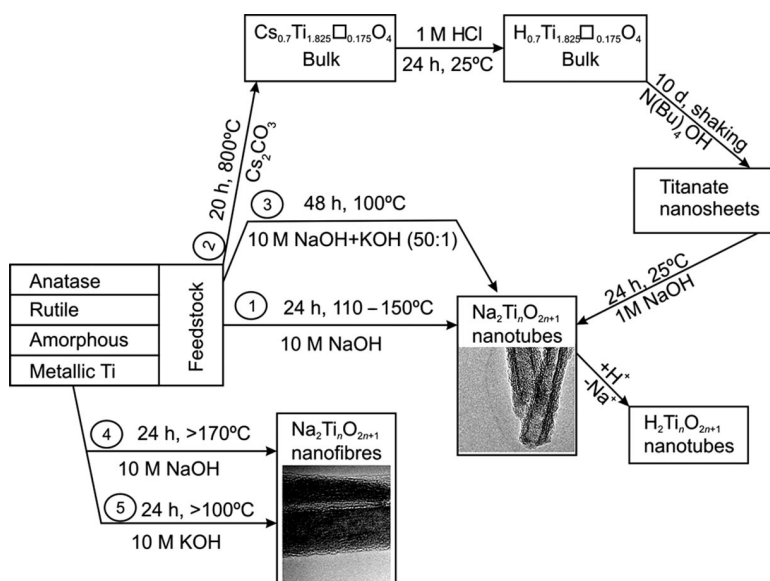


Figure 2. Prospective routes to the manufacture of titanate nanotubes and nanofibres.

In such cases, local overheating of the reaction mixture is possible or a particular form of raw TiO_2 (characterised by a higher rate of dissolution in alkaline solvents) is used.

One of the prospective low-temperature routes to titanate nanotubes is via titanate nanosheets, which can be produced by exfoliation of lepidocrocite-type caesium titanate (see route 2 in Figure 2). The method is based on the phenomenon of spontaneous formation of titanate nanotubes, at room temperature, during the addition of NaOH to a colloidal solution of titanate nanosheets.^[27] The method includes the calcination of TiO_2 with Cs_2CO_3 followed by ion exchange of Cs^+ with H^+ and then exfoliation of titanate nanosheets in the presence of tetrabutylammonium hydroxide (TBAOH) at room temperature.^[28] This route does not require the use of autoclaves, and most of the stages can be readily undertaken under ambient conditions. However, the overall process time and the multistage nature of the process are limitations.

A recently reported approach to reduce the temperature during the synthesis of titanate nanotubes involves the search for a solvent or mixture of solvents, in which, at low temperatures, the concentration of dissolved Ti^{IV} is similar to that in pure NaOH in the temperature range 110–150 °C. This has resulted in a lower-temperature route to the synthesis of nanotubes in a mixture of NaOH and KOH^[29] (route 3 in Figure 2), allowing substantial conversion to be achieved at approximately 100 °C under reflux conditions and at atmospheric pressure. Further improvements to this route would include optimisation of the ratio between NaOH and KOH, lowering the temperature and the use of additives to achieve a high conversion of TiO_2 to titanate nanotubes within several hours under simple reflux conditions.

The formation of titanate nanofibres usually occurs during hydrothermal treatment of TiO_2 raw materials with 10 M NaOH solution at temperatures higher than 170 °C^[16,30] (route 4 in Figure 2). The use of 10 M KOH solution as solvent also results in the formation of nanofibres (route 5 in Figure 2),^[31–33] while a mixture of nanotubes and nanofibres tend to be formed at lower temperatures^[34,35].

2.2. Structure

Identification of the crystal structure of titanate nanotubes has given rise to much debate in the recent literature.^[8,9] In their original work, Kasuga et al. wrongly characterised their product as anatase.^[4] Since then, several possible crystal structures of nanotubular products from the alkaline hydrothermal treatment of TiO_2 have been proposed, including monoclinic trititanates, $\text{H}_2\text{Ti}_3\text{O}_7$,^[36,37] or tetratitanates, $\text{H}_2\text{Ti}_4\text{O}_9$,^[38] orthorhombic titanates, $\text{H}_2\text{Ti}_2\text{O}_4(\text{OH})_2$,^[26] or $(\text{H}_{4-x}\text{Ti}_{2-x}\square_x\text{O}_4\cdot\text{H}_2\text{O})$,^[39,40] monoclinic TiO_2 -(B),^[41] as well as a tetragonal anatase.^[42] The exact determination of crystal structures of nanotubes is still incomplete because of several intrinsic difficulties posed by the nanostructures, including their small crystallite size and the wrapping of the structures along a certain crystallographic axis, both resulting in broadening of the diffraction

signals. The low weight of hydrogen atoms also results in difficulties in locating their precise positions and population inside the crystals.

Recently, more sophisticated crystallographic measurements using total X-ray diffraction and the atomic pair distribution function obtained from synchrotron radiation^[43] have demonstrated that the three-dimensional structure of “ TiO_2 -type” nanotubular materials produced by the alkaline hydrothermal method can be interpreted as an arrangement of TiO_6 octahedrons in corrugated layers. The particular arrangement of octahedrons may depend on the morphology of nanostructures and encapsulation of water or sodium ions. This is also in agreement with the local structure of nanotubes obtained by using extended X-ray absorption fine structure (EXAFS) analysis.^[44] X-ray absorption near-edge spectroscopy (XANES) studies have revealed that the assembly of TiO_6 octahedrons is different from that in anatase, but some anatase-like structures may be present in the nanotubes.^[45]

It is likely that as-synthesised nanotubular materials correspond more closely to sodium titanates rather than anatase or TiO_2 -(B). This is also supported by (1) the frequent observation of a characteristic reflection at small angles in the XRD pattern,^[8] (2) the low isoelectric point (ca. 3) and the negative value of the zeta potential in aqueous solutions due to the acid–base dissociation of titanates,^[46] (3) the preferable adsorption of positively charged ions from aqueous solutions on the surface of nanotubes,^[47] (4) very pronounced ion-exchange properties of nanotubes, allowing almost stoichiometric amounts of alkaline ions to be exchanged^[48] and (5) a dependence of the interlayer distance in the nanotube wall on the amount of alkaline ions inside the nanotube.^[49,50]

The precise crystal structure of titanate nanotubes is still the subject of systematic investigations, including by neutron diffraction studies. It is possible, however, to conclude that the structures have several common features, including a well-defined, layered structure of the wall with a relatively large interlayer distance of approximately 0.7–0.8 nm. An atom of hydrogen situated in these interlayer cavities could be exchanged with alkali metal ions. The layers in the nanotube wall consist of edge- and corner-sharing TiO_6 octahedrons building up to zigzag, corrugated structures.

2.3. Mechanism of Titanate Nanotube Formation

A knowledge of the mechanism of titanate nanotube formation is important, since (1) it allows an improved understanding of how synthesis conditions can affect the morphology of the nanotubes, (2) more convenient conditions can be found for industrial synthesis and (3) it may lead to predictions on the possibility of general mechanistic routes that might be applied to the synthesis of other nanomaterials. Several research groups have studied the mechanism of titanate nanotube formation by using both theoretical (including *ab initio* calculations) and experimental (e.g. microscopic analysis of the intermediate product) methods; these aspects have been reviewed elsewhere.^[7]

There is a general agreement that the reaction proceeds through several stages: (1) slow dissolution of raw TiO_2 accompanied by epitaxial growth of layered nanosheets of sodium titanates, (2) exfoliation of the nanosheets, (3) folding of the nanosheets into tubular structures (seeds), (4) growth of the nanotubes along the axis, (5) exchange of sodium ions by protons during washing and separation of nanotubes.

The appearance of isolated nanosheets during such transformations is crucial to the formation of nanotubes. For example, alkaline hydrothermal treatment of bulk crystals of sodium trititanate $\text{Na}_2\text{Ti}_3\text{O}_7$ at 130 °C did not result in release of nanosheets, and, as a result, no nanotubes were found after 72 h.^[15] In contrast, several days of hydrothermal treatment of sodium titanate in water (without addition of NaOH) at temperatures in the range 140–170 °C resulted in partial H^+ to Na^+ ion-exchange and exfoliation of the isolated nanosheets, which slowly folded into nanotubes of several tens of nanometres in diameter.^[51] A similar process of exfoliation of nanosheets, followed by scrolling into nanotubes, can occur even under slow acidification of nanostructured sodium titanates at 25 °C,^[52] which is also consistent with a room-temperature route for the synthesis of nanotubes (see Figure 2, route 2).^[27] In order to obtain titanate nanotubes, the synthesis conditions should favour the formation of isolated titanate nanosheets.

Computational chemistry calculations suggest that the structure of nanosheets can correspond to anatase^[53–55] or sodium titanate.^[56] The latter is likely to be more stable in an alkaline environment.

The driving force for the curving (scrolling) of nanosheets into nanotubes is suggested to be either the asymmetrical chemical environment on two sides on nanosheet^[57,58] or internal stress arising in multilayered nanosheets from an imbalance in width^[16] occurring during crystallisation. The periodic potential of the crystalline nanosheets can also stabilise the partially curved structures.^[7] The rate of nanosheet curving probably affects the diameter of the nanotubes, but previous studies have not clearly provided (thermodynamic or kinetic) evidence for this.

Under alkaline hydrothermal conditions, nanosheets can also be converted to nanofibres instead of rolling into nanotubes. This usually occurs at temperatures above 170 °C or when KOH is used in place of NaOH. In both cases, the concentration of dissolved Ti^{IV} was found to be similar to, but higher than, that in nanotube synthesis.^[29,34] An increase in the local concentration of Ti^{IV} may result in a faster rate of nanosheet growth with less effect on the rate of nanosheet scrolling. In this case, if the rate of crystallisation is high enough, the thickness of nanosheets can exceed a particular value, when they become too rigid to bend, before curving occurs. This will result in the formation of nanofibres rather than nanotubes.

Energetically, nanofibres are thermodynamically more stable than nanotubes, since the latter have an increased surface area and higher stress within the crystal lattice. It has been reported that long-term alkaline hydrothermal

treatment of TiO_2 ^[59] or overintensification of the synthesis conditions by the use of a revolving autoclave^[23] or microwave radiation^[60] may result in favourable conditions for the formation of nanotubes, but nanofibres can also be formed instead. This suggests that kinetic factors can exert strong control over the route of nanosheet transformation.

2.3.1. Stability and Transformations of Elongated Titanates

In many applications, titanate nanostructures are exposed to chemically aggressive media, which can affect their stability. Therefore, it is important to know the range of operational conditions under which nanotubes are stable or the transformations of nanotubes outside these operational conditions. In Figure 3, transformations resulting in a change of morphology or crystal structures of titanate nanotubes occurring under the influence of various conditions are shown. All transformations can be grouped into three divisions according to the type of treatment, which may be thermal, chemical or mechanical.

Thermal Stability

A knowledge of the thermal stability of titanate nanotubes is important, since some applications or manipulations, including catalyst supports or curing of composite films, require increased-temperature operations. Recent systematic thermal transformation studies of protonated titanate nanotubes^[61] have revealed that annealing of nanotubes in the temperature range 120 °C–400 °C results in slow dehydration of the initial nanotubular $\text{H}_2\text{Ti}_3\text{O}_7$ to nanotubular $\text{TiO}_2\text{-(B)}$ accompanied by a decrease in interlayer spacing in the walls of the nanotubes. This monoclinic $\text{TiO}_2\text{-(B)}$ phase can be detected by using the characteristic reflection in the XRD pattern at ca. 15°.^[7,41] During this topotactic reaction, intermediate phases of $\text{H}_2\text{Ti}_6\text{O}_{13}$ and $\text{H}_2\text{Ti}_{12}\text{O}_{25}$ may be formed. A further increase in the temperature results in the transformation of nanotubular $\text{TiO}_2\text{-(B)}$ to anatase nanorods, which is accompanied by a loss of tubular morphology.

The level of ion-exchanged sodium in nanotubular titanates can determine the thermal stability and the nature of thermal transformations during annealing.^[62–65] When fully saturated with sodium ions, titanate nanotubes can lose their nanotubular morphology and convert to $\text{Na}_2\text{Ti}_6\text{O}_{13}$ nanorods at 600 °C.^[48,66]

Similar thermal transformations can occur in nanofibrous titanates (see Figure 3). Protonated nanofibres can, under calcination, undergo the sequence of transformations to nanofibrous $\text{TiO}_2\text{-(B)}$ at 400 °C, followed by transformation to nanofibrous anatase at 700 °C and then formation of microfibrillar rutile at 1000 °C.^[67,68] The formation of anatase nanofibres is also possible by hydrothermal treatment of titanate nanofibres in water at 150 °C.^[69] The sodium-substituted nanofibres can be converted to $\text{Na}_2\text{Ti}_6\text{O}_{13}$ nanofibres at 500 °C in the presence of hydrogen.^[70]

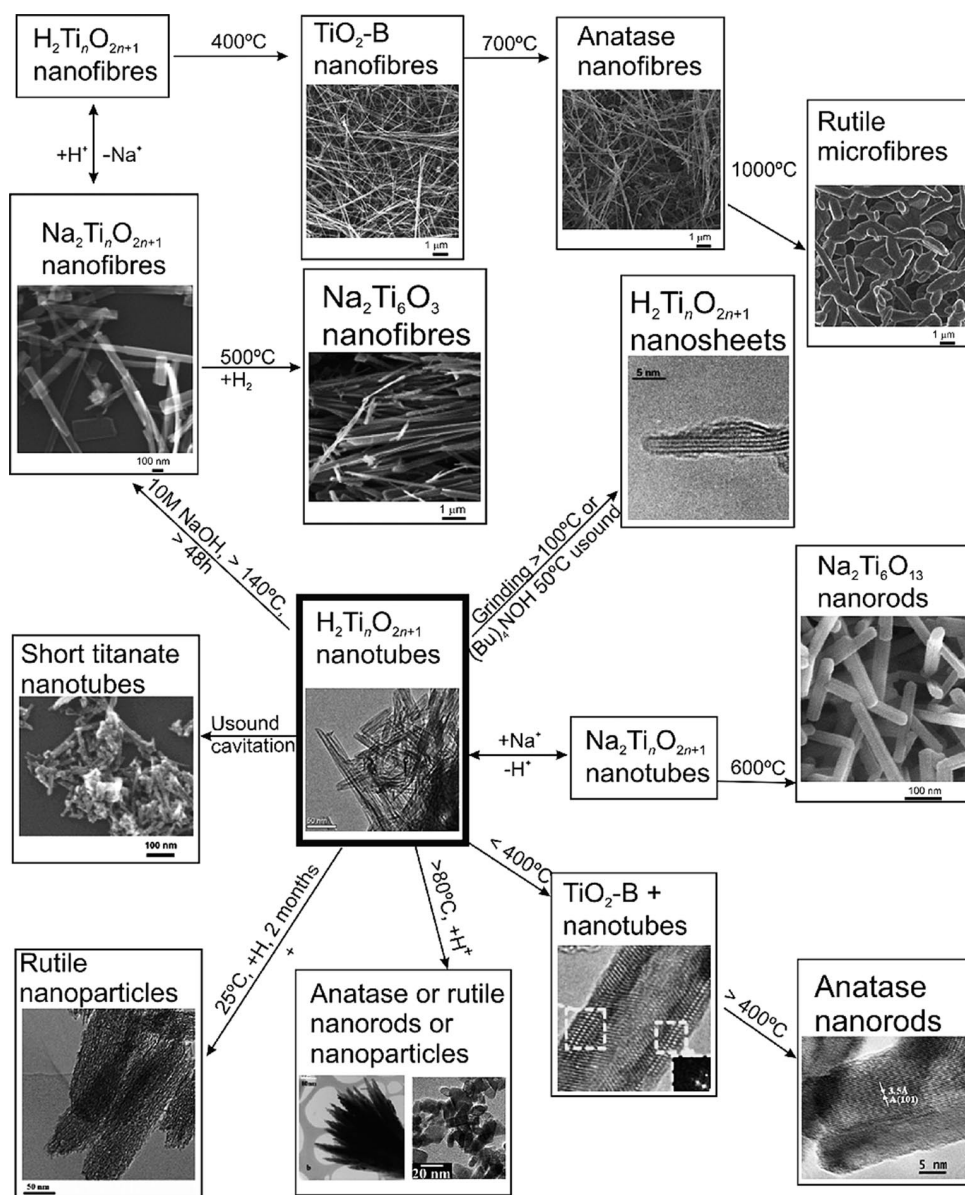


Figure 3. Chemical and structural transformations of titanate nanotubes and nanofibres. The images are taken from refs.^[61,62,67,70,71,73,74] with permission.

Acidic Environments

The phase transformation of titanate nanotubes at elevated temperatures during acid hydrothermal treatment has shown that both the anatase and rutile polymorphs can be formed in the presence of 1 M nitric acid at temperatures higher than 80 °C after 48 h of treatment.^[71] The resulting anatase and rutile polymorphs have nanowire or nanocrystalline morphology. Acidic hydrothermal treatment of titanate nanotubes at 175 °C results in the formation of polycrystalline anatase nanorods.^[72] Titanate nanotubes have poor stability in dilute inorganic acids even at room temperature and slowly transform to rutile nanoparticles over several months. The rate of this transformation de-

pends on the nature of the inorganic acid and is correlated to the solubility of titanates in the acid.^[73]

Titanate nanotubes in their protonated form can be transformed to nanostructured anatase under hydrothermal conditions even in the absence of acid addition.^[74,75] This can be attributed to either a release of acid impurities left after the previous protonation of nanotubes or the lower stability of protonated nanotubes.

It is possible that acid-induced transformation of nanotubes to TiO₂ nanostructures occurs by the dissolution of the initial nanotubes accompanied by the simultaneous crystallisation of TiO₂ nanostructures, since the rate of the transformation is proportional to the steady-state concentration of dissolved Ti^{IV}.^[73]

Mechanical Treatment

Titanate nanotubes and nanofibres are fragile structures that can be readily fragmented by ultrasonic treatment of an aqueous suspension, resulting in a decrease in the average length of the nanotubes or in the splitting and shortening of the nanofibres.^[50] This can provide a convenient tool for controlling the aspect ratio of the nanotubes, allowing, e.g. a reduction in the average length of the nanotubes of up to 50 nm after a 3-h treatment in a conventional ultrasonic bath.

It has recently been shown that the process of nanosheet scrolling into nanotubes can be reversed by mechanical treatment at elevated temperatures. For example, grinding of protonated nanotubes at 100 °C for 45 min resulted in the disappearance of nanotubes and formation of small multilayered nanosheets.^[53] Short-term ultrasonic treatment of titanate nanotubes in the presence of tetrabutylammonium hydroxide (TBAOH) followed by soaking for 3–7 d at 50 °C also results in unwrapping of nanotubes to form nanosheets.^[76]

3. Applications

The properties of elongated morphology, high specific surface area and semiconducting render nanostructured titanates and TiO₂ promising for many applications. The most prominent applications, which include chemical, physical, engineering, mechanical and biomedical ones, are critically reviewed, and gaps in our current knowledge are identified below.

3.1. Reaction Catalysis

Elongated nanostructured titanates are characterised by a relatively high specific surface area measured by nitrogen adsorption, which is typically in the range 200–300 m² g^{−1} for nanotubes and 20–50 m² g^{−1} for nanofibres or nanorods. These values may be contrasted with estimated values, <20 m² g^{−1} for TiO₂ nanotubular arrays produced by anodising, which can be calculated as the geometrical surface area of nanotubes having a characteristic wall thickness (20 nm). The range of pore sizes from 2 to 10 nm ranks titanate nanotubes as mesoporous materials; such structures are widely used in heterogeneous catalytic processes as supports. The high surface area of the support facilitates a high dispersity of the catalyst, while an open mesoporous structure provides an efficient transport of reagents and products.

Protonated titanate nanotubes can provide a moderate acid–base catalyst for esterification^[77] and hydrolysis of 2-chlorethyl ethylsulfide.^[78] The Brønsted acidity of the nanotubular surface can also be increased by treatment with sulfuric acid, to an approximate value of −12.7 on the Hammett scale.^[77] Most of the catalytic studies of titanate nanotubes are, however, focused on the utilisation of its surface as a support for highly dispersed catalysts.

Several methods are used to deposit active catalysts into the pores of titanate nanotubes and nanofibres (see Tables 1, 2, 3 and 4). Incipient wetness impregnation of the catalyst precursor followed by thermal or chemical treatment is a common approach. This method allows the deposition of relatively large quantities of the catalyst; however, the dispersion and the distribution of catalyst is usually inferior to that obtained by using other methods of deposition. A second method is precipitation of the active materials on the surface of the nanotubes, which can be initiated by chemical, photo- or electrochemical treatments. Such methods enable a better distribution of catalyst, but the loading of metal is limited by the amount of precursor adsorbed on the surface of the nanotubes. In addition, there is also the possibility of precursor precipitation in the bulk solution, as a side reaction.

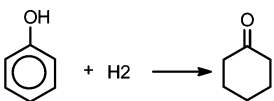
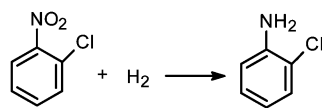
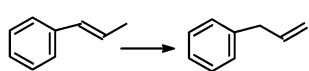
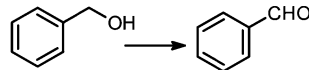
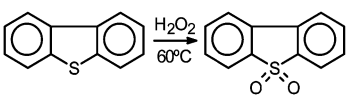
Another *in situ* method for doping titanate nanotubes with catalysts is the addition of a catalyst precursor to the mixture of TiO₂ and aqueous NaOH prior to hydrothermal synthesis. The method allows catalyst atoms to be embedded into the crystal structure of titanate nanotubes. A limitation is that the catalyst loading and dispersion are not easily controlled.

Since titanate nanotubes have good ion-exchange properties,^[48] one method of catalyst deposition involves preliminary ion-exchange of catalyst precursor in the cationic form with protons within nanotubular titanates (see Figure 4). This allows atomic-scale distribution of metal cations in the titanate lattice, achieving higher metal loading relative to adsorption of the precursor on the surface. Washing the sample with clean solvent followed by reduction or chemical treatment avoids precipitation of catalyst in the bulk and results in the formation of clusters or nanoparticles of catalysts evenly distributed only on the surface of the nanotubes. A suitable choice of ionic form for the metal precursor can significantly increase the catalyst loading and maintain a high catalyst dispersity. For example, the use of a diethylenediamine complex of gold {[Au(en)₂]³⁺} instead of the tetrachloroaurate ion ([AuCl₄][−]) results in an increase of more than ten times in the sorption of the gold precursor into the titanate nanotubes.^[79,80]

Examples of various metal catalysts deposited on the surface of titanate nanotubes are shown in Figure 5. The deposition method was ion-exchange followed by chemical treatment. Such an approach can achieve a relatively high catalyst loading while maintaining a relatively small average particle size (see Tables 1, 2, 3 and 4). The metal nanoparticles are deposited on both internal and external surfaces of the nanotubes in the Pd/TiNT, RuOOH/TiNT, Pt/TiNN and Ni/TiNT composites. However, in Au/TiNT and CdS/TiNT composites, the nanoparticles are deposited preferably on the external surface of the nanotubes. Not all catalysts can be deposited by ion-exchange; for example, a suitable cationic form of the precursor may not be available in aqueous solution.

The most widely studied nanotubular supported catalyst is gold (Au/TiNT), resulting from work on Au/TiO₂ catalysts, which are promising for low-temperature CO ox-

Table 1. Reported catalytic processes with nanostructured titanates.^[a]

Catalyst formula	Method of preparation	Particle size /nm	Loading	Process reaction	Activity or performance	Benefits	Ref.
Catalysis							
Au/TiNT	Deposition–precipitation	4–17	0.1–2 wt.-%	$\text{CO} + 0.5\text{O}_2 \rightarrow \text{CO}_2$	$T_{50\%}(\text{°C}) = 47$	Competitive with commercial Au/TiO ₂	[81,82]
Au-Cu/TiNT	Deposition–precipitation	10	1 wt.-%	$\text{CO} + 0.5\text{O}_2 \rightarrow \text{CO}_2$	$T_{50\%}(\text{°C}) = 123$	Conversion Au/TiNT to Au/TiO ₂ NR	[84]
Au/TiO ₂ NR	Deposition–precipitation				$T_{50\%}(\text{°C}) = 77$		
Au/TiNT	Adsorption–reduction	2–5	2–6 wt.-%	$\text{CO} + 0.5\text{O}_2 \rightarrow \text{CO}_2$	$T_{50\%}(\text{°C}) = 70$	Conversion Au/TiNT to Au/TiO ₂ NP	[83]
Au/TiO ₂ NP	Adsorption–reduction				$T_{50\%}(\text{°C}) = 25$		
Au/TiNT	Deposition–precipitation	3–5	1.5 wt %	$\text{CO} + \text{H}_2\text{O} \rightarrow \text{CO}_2 + \text{H}_2$	n/a	Early data show feasibility of catalyst	[87]
Cu ^{II} /TiO ₂ NT	Impregnation or in situ	n/a	2 wt.-%	$6\text{NO} + 4\text{NH}_3 \rightarrow 5\text{N}_2 + 6\text{H}_2\text{O}$	$T_{50\%}(\text{°C}) = 150$	High dispersity of catalyst	[91]
CuO/TiNT	Impregnation calcin. at 200 °C	>5	6 wt %	$\text{CO} + 0.5\text{O}_2 \rightarrow \text{CO}_2$	$T_{50\%}(\text{°C}) = 90$	High activity	[85]
Pd/TiNT	Impregnation–reduction	n/a	1 wt.-%		TOF = 94 h ^{−1} Sel. = 99%	High activity, selectivity and deactivation resistance	[88]
Pd/TiNT	Impregnation–reduction	2–3	1–7 wt.-%		TOF = 186 h ^{−1} Sel. = 84 %	Selectivity can be controlled by Pd size	[89]
Pd(II)/TiNT	Ion-exchange	2–5	10 wt.-%		TOF = 2.3 h ^{−1} Sel. = 93 %	High dispersity of catalyst at high loading	[90]
Pt/TiO ₂ NT	In situ recrystallisation	0.3–3	30 wt.-%	$\text{CO} + 3\text{H}_2 \rightarrow \text{CH}_4 + \text{H}_2\text{O}$	Sel.(CH ₄) = 77%	Higher performance than that of Pt/TiO ₂	[96]
Pt/TiNT	Adsorption–photoreduction	2	2 wt.-%	$\text{CO} + \text{H}_2\text{O} \rightarrow \text{CO}_2 + \text{H}_2$	TOF = 20 h ^{−1}	Early data shows feasibility of catalyst	[86]
Au/TiNT	Adsorption–photoreduction	10		$\text{CO}_2 + 3\text{H}_2 \rightarrow \text{CH}_3\text{OH} + \text{H}_2\text{O}$	n/a		
Ru ^{III} /TiNT	Ion-exchange–alkali treatment	1–2	1–9 wt.-%		TOF = 450 h ^{−1} Sel. = 99	High dispersity of catalyst at high loading	[92]
TiNT	Hydrothermal	n/a	n/a	$\text{C}_2\text{H}_5\text{SC}_2\text{H}_4\text{Cl} + \text{H}_2\text{O} \rightarrow$	n/a	Feasibility of titanate Nanotubes in hydrolysis	[78]
WO _x /TiNT	Impregnation–calcin. at 500°C	<1	5–20 wt.-%	$\text{C}_2\text{H}_5\text{SC}_2\text{H}_4\text{OH} + \text{HCl}$	TOF = 54 h ^{−1}	Route to obtain highly dispersed WO _x on TiO ₂	[93]
WO _x /TiO ₂ NF							

[a] TiNT: titanate nanotubes, TiNF: titanate nanofibres, NR: nanorods, NP: nanoparticles, n/a: not available.

dation.^[81,82] The early Au/TiNT catalysts have demonstrated an activity comparable to standard Au/TiO₂ materials. Recent improvements in performance have been attempted by acid-assisted transformation of nanotubes (with deposited gold) to TiO₂ nanoparticles^[83] or by high-temperature transformation of gold particles on nanotubes to those on nanorods.^[84] Some successful attempts to reduce the use of precious metals such as gold have also been made by using CuO^[85] or Cu-Au^[81] composites deposited on the surface of titanate nanotubes.

Catalysts made from gold deposited on titanate nanotubes have also demonstrated high activity for CO₂ reduction by hydrogen^[86] and water shift reactions.^[87] Most of these catalysts were prepared by precipitation from

HAuCl₄ solution when dispersity and the loading of gold nanoparticles is difficult to control. Further improvements in catalyst preparation by utilising the ion-exchange method could possibly improve the activity of catalysts.

The catalytic activity of palladium nanoparticles (in metal or metal hydroxide form) deposited on the surface of titanate nanotubes or nanofibres has been studied for the hydrogenation of phenol to cyclohexanone,^[88] hydrogenation of *ortho*-chloronitrobenzene to *ortho*-chloroaniline^[89] and isomerisation of allylbenzene (double bond migration)^[90] (see Table 1). Copper(II) catalysts embedded into titanate nanotubes in situ followed by conversion to TiO₂ nanotubes by calcination showed good activity and selectivity for the catalytic reduction of NO.^[91] Catalytic studies of

Table 2. Reported electrocatalytic processes with nanostructured titanates.^[a]

Catalyst formula	Method of preparation	Particle size / nm	Loading	Process reaction	Activity or performance	Benefits	Ref.
Electrocatalysis							
Au/TiNT	Ion-exchange–reduction	4	0.1 mg cm ^{−2}	$\text{BH}_4^- + 8 \text{OH}^- - 8\text{e}^- \rightarrow \text{BO}_2^- + 6 \text{H}_2\text{O}$	8320 mC mg ^{−1} cm ^{−2}	Borohydride fuel cell	[100]
Pd/TiNT	Ion-exchange–reduction	n/a	3 wt.-%	$\text{CH}_3\text{OH} - 6\text{e}^- + \text{H}_2\text{O} \rightarrow \text{CO}_2 + 6\text{H}^+$	n/a	Methanol fuel cell catalysts	[97]
Pd/TiNT	Ion-exchange–reduction	6–13	0.5 mg cm ^{−2}	$\text{N}_2\text{H}_4 - 4\text{e}^- \rightarrow \text{N}_2 + 4\text{H}^+$	n/a	More active than Pd/TiO ₂ NP	[123]
Pd/TiO ₂ NR + C	Coprecipitation–reduction	30	0.3 mg cm ^{−2}	$\text{C}_2\text{H}_5\text{OH} - 12\text{e}^- + 3\text{H}_2\text{O} \rightarrow 2\text{CO}_2 + 12\text{H}^+$	n/a	TiO ₂ + carbon composite improves conductivity	[98]
RuO ₂ /TiNT	Impregnation	n/a	n/a	$\text{CO}_2 + 5\text{H}_2\text{O} + 6\text{e}^- \rightarrow \text{CH}_3\text{OH} + 6\text{OH}^-$	Current yield = 60%	Better performance relative to RuO ₂ /TiO ₂	[122]
TiNT + Pt/C	Mixing in slurry	2	1 mg cm ^{−2}	$\text{C}_2\text{H}_5\text{OH} - 12\text{e}^- + 3\text{H}_2\text{O} \rightarrow 2\text{CO}_2 + 12\text{H}^+$	120 mA mg ^{−1} (Pt)	TiNT promotes Pt/C activity, tolerance to CO	[99]

[a] TiNT: titanate nanotubes, TiNF: titanate nanofibres, NR: nanorods, NP: nanoparticles, n/a: not available.

Table 3. Reported supercapacitor processes with nanostructured titanates.^[a]

Catalyst formula	Method of preparation	Particle size / nm	Loading	Process reaction	Activity or performance	Benefits	Ref.
Supercapacitor							
RuO ₂ /TiNT	Precipitation	n/a	4–21 wt.-%	$\text{RuO}_2 + \text{H}_2\text{O} + \text{e}^- \rightarrow \text{RuOOH} + \text{OH}^-$	230 F g ^{−1}	Early reports	[125,126]
VO _x /TiNF	Adsorption	n/a	n/a	$\text{VO}_2^+ + 2\text{H}^+ + \text{e}^- \rightarrow \text{VO}^{2+} + \text{H}_2\text{O}$	n/a	Capacitance is higher than that for bulk V ₂ O ₅	[124]
Co(OH) ₂ /TiNT	Precipitation	n/a	25–75 wt.-%	$\text{Co(OH)}_2 + \text{OH}^- \rightarrow \text{CoOOH} + \text{H}_2\text{O} + \text{e}^-$	229 F g ^{−1}	Capacitance is higher than that for bulk Co(OH) ₂	[128]
Ru _{1−y} Cr _y O ₂ /TiNT	Coprecipitation	n/a	4–23 wt.-%	$\text{Ru}_{1−y}\text{Cr}_y\text{O}_2 + \text{H}_2\text{O} + \text{e}^- \rightarrow \text{Ru}_{1−y}\text{Cr}_y\text{OOH} + \text{OH}^-$	250 F g ^{−1}	Lower cost than that for pure RuO ₂	[127]
Co(OH) ₂ + Ni(OH) ₂ /TiNT	Coprecipitation	n/a	60 wt.-%	$(\text{CoNi(OH)})_2 + \text{OH}^- \rightarrow (\text{CoNiOOH}) + \text{H}_2\text{O} + \text{e}^-$	631 F g ^{−1}	High capacitance	[129]

[a] TiNT: titanate nanotubes, TiNF: titanate nanofibres, NR: nanorods, NP: nanoparticles, n/a: not available.

hydrated forms of ruthenium(III) deposited by ion exchange on the surface of titanate nanotubes in the selective oxidation of alcohols have revealed the independence of specific catalytic activity on catalyst loading.^[92] This is consistent with electron microscope observations showing that an increase in catalyst loading results in an increase in the density of catalyst particles on the surface rather than an increase in the size of the particles.

Potential catalysts of selective oxidation of dibenzothiophene with hydrogen peroxide at 60 °C are WO_x/TiO₂ nanostructures obtained by calcination of titanate nanotubes impregnated with (NH₄)₂WO₄.^[93] This reaction models the process of desulfurisation of oils, and the catalyst demonstrates a high activity. During the preparation of the catalyst, an interesting transformation in morphology has been reported.^[94] The calcination of titanate nanotubes impregnated with (NH₄)₂WO₄ at 500 °C results in the collapse of the tubular structure accompanied by the release of residual Na⁺ ions onto the surface of fibrous anatase, leading to the formation of highly dispersed Na_x(WO₄) nanoparticles in which tungsten is in tetrahedral coordination, which provides a high activity for selective oxidation.

Platinum deposited on the surface of wide-pore nanotubular catalyst supports can be synthesised by using the [Pt(NH₃)₄](HCO₃)₂ complex as a template.^[95] In this method, the template is also a catalyst precursor. Such Pt/TiO₂ nanotubular catalysts can be characterised by their wide diameter (100–200 nm) and the well-dispersed Pt nanoparticles on the nanotubular surfaces with a high loading. These catalysts show a good performance both in the selective reduction of CO with H₂ to form CH₄ and in the water shift reaction.^[96]

All reported applications of titanate nanotubes in catalysis emphasise the benefits of a high surface area together with the versatility of the surface chemistry and electronic interactions between catalyst and support, which improve catalytic activity. The low cost of titanate nanotubes opens a novel route for nanostructured TiO₂-supported catalysts by using either acid or thermal transformations. The control of localisation of the catalyst (either inside or outside the hollow tube) is still challenging.^[79] This is an important topic for further studies on size-selective catalysts, which can utilise the geometry of cylindrical pores of 3–8 nm in diameter and avoid the formation of bulky side products.

Table 4. Reported photocatalytic processes with nanostructured titanates.^[a]

Catalyst formula	Method of preparation	Particle size / nm	Loading	Process reaction	Activity or performance	Benefits	Ref.
Photocatalysis							
Pt/TiO ₂ -(B) NT-anatase NP	Calcination at 400 °C	10 nm (anatase)	1 wt.-% Pt, 33% TiO ₂ (B)	CH ₃ CH ₂ OH + <i>hν</i> → CH ₃ CHO + H ₂	20% higher than that of Pt/P25	Facile method to bicrystalline catalyst	[146]
Cr ^{III} /TiO ₂ NP	Hydrothermal acid of Cr-TiNT	5 nm	3 wt.-%	H ₂ O + <i>hν</i> → H ₂ + O ₂	n/a	Novel route for ion implantation	[155]
TiO ₂ NP (anatase)	Calcination H-TiNT	n/a	n/a	Photocatalytic oxidation of organics	Higher than that of P25	Novel route for anatase nanoparticles	[140]
TiO ₂ NR (anatase)	Calcination H-TiNT	10 × 100 nm	n/a	Photocatalytic oxidation of organics	Higher than that of P25	Novel route for anatase nanorods	[46,141]
Pt/TiNT	Photodeposition	n/a	1 wt.-%	CH ₃ CH ₂ OH + <i>hν</i> → CH ₃ CHO + H ₂	n/a	Early data on photodehydrogenation	[165]
CdS/TiNT	Ion-exchange surface reaction	6 nm	n/a	Dye oxidation	n/a	Photosensitisation of TiNT	[156,157]
N-doped TiO ₂ NP	Calcination with NH ₃ (gas)	10 nm	1% (N)	2C ₃ H ₆ + 9O ₂ → 6CO ₂ + 6H ₂ O	Three times higher than that of N-P25	Photosensitisation to visible light	[152]
TiNT	Microwave	n/a	n/a	NH ₄ ⁺ + O ₂ → NO ₂ ⁻ + NO ₃ ⁻	Less than that of P25	Good adsorption of NH ₃	[138]
NiO/TiNF; TiNF	Impregnation	n/a	0.2 wt.-%	CHCl ₃ oxidation	Higher than that of P25	Accommodation of Ni in tunnel structure	[160]
TiO ₂ /TiNF	Epitaxial growth by precipitation	10–50 nm	n/a	Dye oxidation	Higher than that of TiNF	Support for photocatalyst	[147]
TiO ₂ NF, TiO ₂ NP	Acid treatment of TiNF at 180 °C	n/a	n/a	Dye oxidation	Comparable with that of P25	Novel route for nanostructured anatase	[144]
Pt/TiNT	Sputtering	n/a	n/a	H ₂ O + <i>hν</i> → H ₂ + O ₂	Higher than that of TiO ₂	Early data showing water splitting	[163]
SnTTP/TiNF	In situ intercalation	n/a	n/a	Dye oxidation	n/a	Synergy in using UV + visible light	[161]
TiNF, TiO ₂ -(B) NF, anatase NF	Calcination	n/a	n/a	CH ₃ OH + <i>hν</i> → HCHO + H ₂	Higher than that of P25	Systematic comparison of elongated structures	[164]
Bi ₂ Ti ₂ O ₇ NT	AAO template	0.2 μm × 7 μm	n/a	Dye oxidation	Higher than that of bulk Bi ₂ Ti ₂ O ₇	Effect of dimension on the activity of catalyst	[162]

[a] TiNT: titanate nanotubes, TiNF: titanate nanofibres, NR: nanorods, NP: nanoparticles, n/a: not available, P25: spheroidal TiO₂ nanoparticles (Degussa).

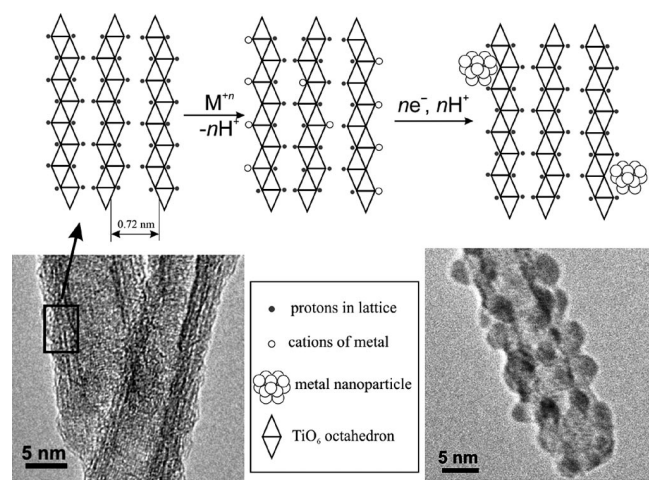


Figure 4. Ion-exchange-assisted deposition of Pd nanoparticles on the surface of titanate nanotubes.

3.2. Electrocatalytic Storage or Generation of Electricity

Titanate nanotubes have relatively good proton^[59] and moderate electron conductivities; the latter is higher than that for anatase,^[7] making titanate nanotubes a possible

candidate for the realisation of composite nanostructured electrodes. All reported applications of nanostructured elongated titanates in electrochemical processes can be divided into areas such as fuel cell technology, lithium batteries, supercapacitors and general electrocatalysis.

3.2.1. Fuel Cells and Batteries

During the last two decades, enormous developments in fuel cell technologies have taken place as a result of concerns over the insufficient efficiency of and environmental problems related to existing energy converters. The nanostructured titanates and TiO₂ have been considered as supports for electrocatalysts of fuel oxidation (see Figure 6a). Early studies of palladium nanoparticles deposited on the surface of titanate nanotubes demonstrated the feasibility of nanostructured titanates for oxidation of methanol in liquid fuel cells.^[97] Further improvements in catalyst performance have been achieved by increasing the electroconductivity of the elongated Pd/TiO₂ nanorods coated with carbon by calcination of nanotubes coated with poly(ethylene glycol) at 600 °C.^[98]

Recent studies also showed that simple addition of titanate nanotubes to the standard Pt/C catalyst by mixing in

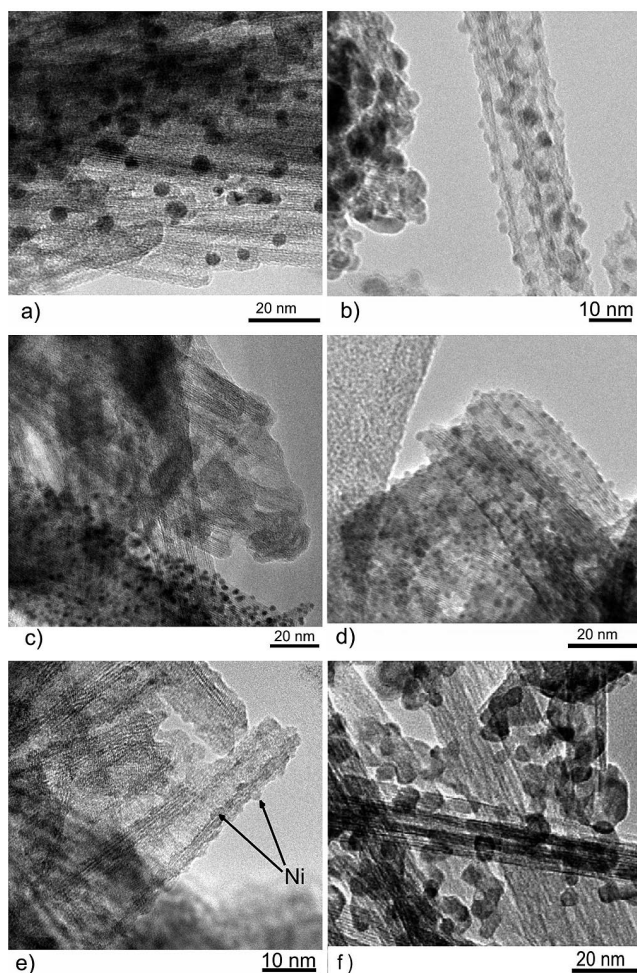


Figure 5. Examples of titanate nanotubes decorated with metal nanoparticles, which are used in catalysis: (a) Au/TiNT, (b) Pd/TiNT, (c) Pt/TiNT, (d) RuOOH/TiNT, (e) Ni/TiNT and (f) CdS/TiNT. Images (a), (c) and (d) are taken from ref.^[180] while image (f) is taken from ref.^[159] with permission.

slurry followed by drying on the surface of the electrode results in the enhancement of catalyst performance due to the structural water in the nanotubes and the increase in the resistance to CO poisoning by stimulation of its desorption from the catalyst surface.^[99] Gold deposited onto titanate nanotubes has also demonstrated a better performance than commercial Au/C catalysts for the anodic oxidation of NaBH₄ in the direct borohydride fuel cell^[100] (see Figure 6b). The electrical charge during oxidation of the borohydride ion per unit mass of gold was approximately 8300 mC cm² mg⁻¹ (see Table 2) and 3900 mC cm² mg⁻¹ for Au/TiNT and Au/C electrocatalysts, respectively.

Titanate nanotubes have been used not only for the enhancement of fuel cell catalyst efficiency but also for improved proton conductive membrane performance. Addition of titanate nanotubes up to 15 wt.-% to the Nafion membrane was shown to enhance proton exchange conductivity at elevated temperatures (130 °C) as a result of water retention in the nanotubular titanates.^[101] Such a composite

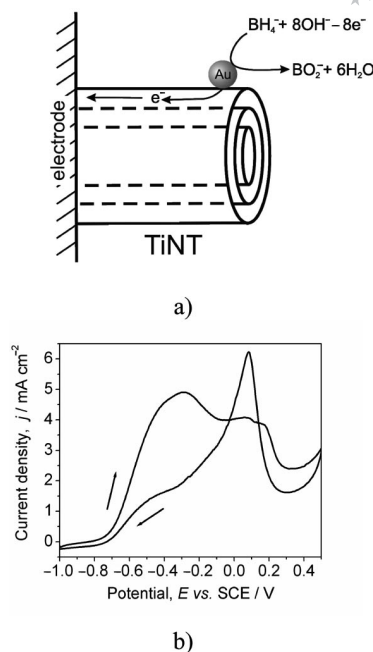


Figure 6. Applications of titanate nanotubes in fuel cell electrodes: (a) schematics of the electron transport process in the direct borohydride fuel cell, (b) a cyclic voltammogram for the oxidation of the borohydride ion at an Au/TiNT electrode.^[100]

membrane can be cast from a mixed slurry of nanotubes with 5% Nafion solution (DuPont) redissolved in dimethyl sulfoxide.^[101]

3.2.2. Lithium Batteries

Nanostructured materials are widely used as electrodes in rechargeable lithium batteries.^[102] Elongated titanates also attract attention as possible negative electrode materials for lithium cells because of their open, mesoporous structure, efficient transport of lithium ions and effective ion-exchange properties, which result in a high value of charge/discharge capacity (<300 mA h g⁻¹) and fast kinetics together with high robustness and good safety characteristics.^[7,103] These new electrodes can replace commercial carbon negative electrodes, which suffer from safety concerns (electroplating of lithium) and the formation of a solid-electrolyte interface (SEI) layer that leads to charge loss.

Figure 7a shows the principle of lithium storage in nanotubular titanates. During charging, lithium ions from the electrolyte solution intercalate between layers of the wall along the axis of the nanotubes.^[50] They then form the Li_xTiO₂ phase after cathodic reduction. The charge capacity of lithium batteries depends on the availability of the lithium reduction sites, and the power characteristics of the batteries are often governed by the kinetics of lithium intercalation.

There are three consecutive steps in the process of charging/discharging the electrode, namely: (1) diffusion of lithium ions in the electrolyte, (2) diffusion of intercalated ions/atoms and (3) electrochemical reaction. Each of these stages, as well as electron transport, can be limiting in the

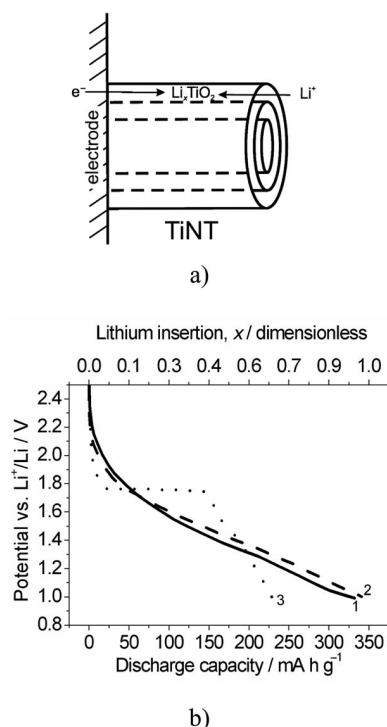


Figure 7. Applications of titanate nanotubes involving lithium storage: (a) the principle of electrochemical lithium storage in a battery; (b) the first discharge curve of (1) TiNT, (2) $\text{TiO}_2(\text{B})$ NT and (3) TiO_2 NR. (Adapted from ref.^[111]).

overall process. The use of nanostructured titanates and TiO_2 significantly improves the rate of the diffusion of intercalated lithium ions because of their small size and the featured crystal structure of the material, which provides sufficient space (interlayer spacing in the wall) for ionic transport.

At the present time, the following elongated nanostructures have been studied for lithium storage: titanate nanotubes^[104–106] (TiNT), titanate nanofibres^[107–110] (TiNF), $\text{TiO}_2(\text{B})$ nanotubes^[41,111] nanofibres^[112–114] and TiO_2 (anatase) nanorods.^[111,115] The last three nanostructures were obtained by calcination of the protonated forms of the corresponding titanates (see Figure 3). All of these structures demonstrate an impressive ability to store lithium ions (see Table 5).

Titanate nanotubes are characterised by a high initial discharge capacity, which quickly decreases from ca. 300 to ca. 180 mAh g^{-1} within several cycles. The charge/discharge curves are characterised by the absence of a constant cell voltage plateau. Slightly better cycling stability was observed when using titanate nanofibres, which showed similar values of lithium storage capacity. Although these nanostructures have different morphologies and typical sizes, the rate of lithium ion intercalation is relatively fast in both nanostructures, as seen in the pseudocapacitive, faradaic behaviour.^[105,109] This apparent inconsistency can be explained by taking into account the direction of alkaline ion flow in nanotubes and nanofibres. It was suggested that alkaline ions diffuse along the length of titanate nanotubes, whereas they can diffuse in a direction perpendicular to the length of nanofibres.^[50] The characteristic length of nanotubes and width of nanofibres are several hundreds of nanometres, resulting in a characteristic diffusion time of the intercalated lithium ions in both of these nanostructures: ca. 30 min.

The mechanism of lithium diffusion in $\text{TiO}_2(\text{B})$ nanotubes and nanofibres is probably different from that in titanates, since, instead of diffusing between the layers of titanates, the lithium ions diffuse inside the smaller-size tunnels in the $\text{TiO}_2(\text{B})$ crystals.^[113] Besides, because of the absence of ion-exchanged protons, the side reaction, that is,

Table 5. Summary of electrodes containing elongated titanate or TiO_2 nanoparticles used for lithium storage.

Electrode	Discharge capacity / $\text{mAh g}^{-1[\text{a}]}$	Specific current density / mA g^{-1}	Merits for lithium storage	Ref.
TiNT	220–250	110, 200	Higher capacity than that of P25 ^[b]	[104]
TiNF	170	2000		
	220	110	Higher capacity than that of P25	[107]
	190	300		[108]
	130	2500		[109]
$\text{TiO}_2(\text{B})$ NT	240	50	Higher capacity than that of P25	[111]
$\text{TiO}_2(\text{B})$ NF	200	200	Higher capacity than that of P25	[112,113]
	100	2000		
TiO_2 (anatase) NR	190	50	Plateau in current vs. potential curve	[111,115]
	240	36		
$\text{NiO/TiO}_2(\text{B})$ NT	240	100	Durability, lower electrical resistance	[118]
	170	2000		
C- TiO_2 (anatase) NR	204	70	Lower resistance, plateau in current vs. potential curve	[116]
Co-TiNF	350	50	Intercalated Li affects magnetic properties	[117]
Co- TiO_2 (anatase) NF	140	50		
Ag/TiNT	190	50	Higher cycling stability at higher discharge rate	[119]
	160	600		
Sn/TiNT	312	30	SnLi alloying in pores of TiNT	[120]
$\text{TiO}_2(\text{B})$ NT	296	25	Effect of electrode thickness on the discharge kinetics	[121]
TiO_2 (anatase) NR	215	25		

[a] After ten cycles. [b] P25: spheroidal TiO_2 nanoparticles (Degussa).

the hydrolysis of the electrolyte, is suppressed. As a result, the initial discharge capacity does not deteriorate quickly, and the cycling stability is slightly better than that in nanostructured titanates. After a few cycles, the lithium storage capacity is similar to that in nanostructured titanates, and the pseudocapacitive current behaviour also suggests that diffusion of lithium (external in the electrolyte and internal in the intercalated state) is not the limiting stage.

The anatase nanorods produced by calcination of TiNT are characterised by a lower discharge capacity (see Table 5), a characteristic plateau in the charge/discharge curve (see Figure 7b) and good reversibility. For all elongated nanostructures, the coulombic efficiency was close to 100%.

The power output demand for new-generation lithium batteries is stimulating their use at higher current densities, which places additional requirements on the electroconductivity of the nanostructured titanates and TiO_2 electrodes. Recent approaches to improve the conductivity of elongated structures include doping of TiO_2 nanorods with carbon,^[116] doping of TiNF and TiO_2 NF with cobalt,^[117] deposition of NiO particles on the surface of TiO_2 -(B) nanotubes,^[118] coating the surface of TiNT with silver nanoparticles^[119] and coprecipitation of a tin phase in the pores of TiNT.^[120] All of these methods reduce the electrical resistance of the electrode, improve durability and decrease charge capacity degradation during high charge/discharge rate trials.

Another important issue for high-current lithium batteries is the resistance due to the limited mass transport of lithium in the electrolyte resulting in reduced voltage of the cell at high current densities for thick electrodes.^[121]

Further improvements in the performance of the lithium cell will probably focus on improvements of (1) the electroconductivity of the elongated nanostructures, (2) mass transport of lithium ions in the electrolyte by optimal design of electrode porosity, (3) charge capacity of the electrode and (4) cycling stability of the electrode.

3.2.3. Supercapacitors and General Electrochemistry

Composite electrodes consisting of titanate nanotubes supporting nanoparticles of precious metals have also been studied for electrocatalytic processes including the electrochemical reduction of CO_2 to methanol with a RuO_2 /TiNT composite electrode^[122] and oxidation of hydrazine (N_2H_4) by using palladium-decorated titanate nanotubes.^[123] In both cases, the composite electrodes demonstrated a better performance than TiO_2 -based ones.

The oxides of transition metals, which can have several valence states, are prospective materials for the storage of electrical energy in electrochemical capacitors. Effective dispersion of these oxides on the electrode surface is critical to achieve a high capacitance, which can be accomplished by using titanate nanotubes as a support for the metal oxide. Early reports of vanadium(V) oxide deposited on the surface of titanate nanotubes showed the feasibility of such composites as capacitors.^[124] Further improvements of the capacitance stimulated the use of ruthenium (RuO_2)^[125,126]

or mixed ruthenium/chromium oxides ($\text{Ru}_{1-y}\text{Cr}_y\text{O}_2$)^[127] deposited on the surface of titanate nanotube composites, facilitating a high specific (per mass of Ru/Cr oxide) capacitance of ca. 1272 F g^{-1} for 4 wt.-% of $\text{Ru}_{1-y}\text{Cr}_y\text{O}_2$ loading (see Table 3). This value is almost two times higher than the electrochemical capacitance of bulk $\text{Ru}_{1-y}\text{Cr}_y\text{O}_2$ positive electrode. The high cost of ruthenium has encouraged the search for lower-cost substitute elements, resulting in the synthesis of cobalt hydroxide^[128] and cobalt nickel double hydroxide deposited on TiNT, having a specific (per mass of metal oxide) capacitance of approximately 1000 F g^{-1} .^[129]

3.3. Photocatalysis in Elongated Titanates

During the last three decades, titanium dioxide has been comprehensively studied as a wide-band-gap photocatalyst for the oxidation of organic compounds.^[3] The best TiO_2 -based catalysts are usually characterised by a highly crystalline structure, which can reduce recombination of photo-generated carriers, a high specific surface area, for acceleration of the interfacial reaction rate, and abundance of surface OH groups, required for the generation of OH radicals during photocatalytic reactions. All of these features are intrinsic to elongated titanates.

The optical properties of titanate nanotubes have been recently studied by various methods. The absorption threshold determined from diffuse reflectance spectra is usually very close to the band gap of titanium dioxide,^[130] which is ca. 3.2 eV. However, more accurate studies of diluted colloidal solutions of TiNT, which avoid the errors caused by elastic light scattering, estimated the band gap of the nanotubes as ca. 3.87 eV,^[131] which is wider than that of TiO_2 and closer to that of titanate nanosheets (3.84 eV^[132]). Photoluminescence measured at -196°C from the powder state samples usually shows a band at 2.4 eV,^[133] whereas the spectrum of nanotubes dispersed in water^[131] shows a multiple-line spectrum with several characteristic bands at 3.99, 3.77, 3.54, 3.09, 2.94, 2.51, 2.38, 2.16, 2.08 and 1.99 eV. Discrepancies between these two methods are probably due to the strong scattering of light from solid powder samples, which can mask the photoluminescence signals.

Absorption of light by titanate nanotubes results in the generation of charge carriers, which can eventually relax into a single electron trapped oxygen vacancy (SETOV)^[134] or be trapped by Ti^{4+} ions to form Ti^{3+} centres, which can cause visible light absorption. Transient studies of photo-generated charged carriers in titanate and TiO_2 -(B) nanotubes have revealed that the lifetime of trapped electrons is extended, relative to that of TiO_2 nanoparticles, suggesting an improved charge separation due to the elongated morphology.^[135]

It is well known that Na^+ impurities can significantly decrease the photocatalytic activity of TiO_2 by acting as recombination centres.^[3] The high amount of sodium ions retained in titanate nanostructures after alkaline hydrothermal synthesis can also significantly reduce the photocatalytic activity of titanates. This was recently confirmed by

the observation of the negative effect of sodium content on the photocatalytic activity of titanate nanotubes during the oxidation of dyes.^[136,137] In contrast, the removal of sodium ions by protonation of titanate nanotubes results in luminescence quenching,^[130] meaning that centres of radiative recombination are associated with sodium sites, which is consistent with the observation of the negative effect of sodium ions on the photocatalytic activity of TiNT.

The photocatalytic activity of as-prepared titanate nanotubes was found to be smaller (but not zero) than the activity of the standard P25 catalyst in the oxidation of NH_3 ^[138] as well as in the oxidation of dyes in aqueous suspensions.^[139] This can be attributed to either impurities of sodium or moderate crystallinity of as-prepared titanate nanotubes. Further improvements of activity were directed to the transformation of the initial nanotubes to the more photocatalytically active forms of TiO_2 .

Two methods for H-TiNT transformation have been reported, namely heat and combined heat/acid treatments. The anatase nanoparticles^[140] or nanorods^[46,136,141,142] produced by calcination of H-TiNT at 400 °C were characterised by better photocatalytic activity in the oxidation of various organic molecules or dyes than that of initial H-TiNT. The increase in photocatalytic activity was accompanied by improvement of nanostructure crystallinity. A further increase in calcination temperature resulted in a lower photocatalytic activity due to stripping of the surface OH groups and reduction in the surface area of nanostructures. In contrast, the acid hydrothermal treatment of H-TiNT with residues of HCl at 200 °C^[143] or H-TiNF with 0.1 M HNO_3 (pH 0–7) at 180 °C^[144] results in the formation of nanostructured anatase with a fibrous or particulate morphology, which showed good photocatalytic activity for the oxidation of model organic dyes. The method of acid hydrothermal transformation promises a reduction in synthesis temperatures and helps retain the surface OH groups intact.

Additional improvement of charge separation in elongated titanates can be achieved by using the recently discovered synergetic effect in mixed-phase nanocomposites occurring between two crystal forms of TiO_2 (anatase and rutile) due to the small difference in flat band potentials, which stimulates spatial separation of carriers, reducing their recombination.^[145] The bicrystalline mixture of 33% TiO_2 -(B) nanotubes and 67% anatase nanoparticles prepared by calcination of H-TiNT is characterised by an improved photocatalytic activity relative to P25 TiO_2 for hydrogen evolution from ethanol.^[146] This approach has also demonstrated the versatility of this method, which enables the easy preparation of mixed-phase nanocomposites. Titanate nanofibres^[147] and nanotubes^[148] decorated with TiO_2 (anatase) nanoparticles deposited by hydrolysis of TiF_4 in the presence of H_3BO_3 are also characterised by good surface adhesion, an increased surface area and improved photocatalytic activity.

Although TiO_2 -based photocatalysts are very active in photocatalytic reactions, the major drawback delaying their wide industrial use is the relatively short wavelength of the

light necessary for the photocatalytic reaction. The sensitisation of the photocatalyst to visible light is a “holy grail”. Several approaches to sensitisation of elongated titanate and TiO_2 nanostructures have been recently explored.

One of the successful ways to sensitise TiO_2 to visible light is to dope it with nitrogen, forming additional levels in the forbidden zone of the wide-band-gap TiO_2 . Several methods of doping titanate nanotubes with nitrogen were reported. The first is the ion exchange of ammonium (NH_4^+) ions with protons in H-TiNT followed by the calcination of the sample in air at 400 °C, resulting in the formation of N-doped TiO_2 -(B) nanotubes.^[149,150] The alkaline hydrothermal treatment of preliminary doped TiO_2 with nitrogen also results in the formation of N-doped titanate nanotubes.^[151] The third method is nitration of TiNT with gaseous NH_3 at temperatures in the range 400–700 °C^[152] at atmospheric pressure. The last method allows control over the level of N-doping at a nitrogen surface concentration of up to 12%. All N-doped elongated nanostructures show good photocatalytic activity in the visible range of incident light. The nature of photoactive centres in N-doped elongated titanates and TiO_2 is being actively studied. The recent X-ray photoelectron spectroscopy (XPS) and ESR data shows that nitrogen in the form of NO probably occupies the interstitial positions between the oxygen vacancy and Ti^{4+} , forming a visible light absorption centre, which is energetically positioned within the band gap of TiO_2 . The photocatalytic activity in the visible range correlates with the concentration of these centres and is higher for N-doped anatase nanorods obtained by nitration of H-TiNT than N-doped P25 prepared at 600 °C.^[152]

Another method to sensitise TiO_2 to visible light is implantation with Cr^{III} ions,^[153] where Cr^{3+} ions occupy the positions of Ti^{4+} in the lattice and form electron levels in the forbidden zone. Photocatalytic activity under visible light is observed for catalysts with isolated Cr^{3+} ions inside the TiO_2 lattice. The agglomeration of chromium ions at higher chromium loading results in the appearance of recombination centres and a decrease in activity. There are several reports on the doping of titanate nanotube photocatalysts with chromium. Low levels of chromium doping (0.5 wt.-%) in titanate nanotubes can be achieved by alkaline hydrothermal treatment of preliminarily Cr-doped anatase.^[154] Such a photocatalyst showed some activity under visible light during dye oxidation. The acid-assisted hydrothermal transformation of H-TiNT to anatase at 240 °C over 24 h in the presence of 0.1 M HNO_3 and chromium(III) results in the formation of Cr-doped anatase nanoparticles,^[155] in which the level of chromium can be varied up to 10 wt.-%. However, the most active catalyst for photoelectrochemical water splitting was found to be a catalyst having 3 wt.-% loading, in which no formation of the Cr_2O_3 phase is observed.

Several attempts to decorate titanate nanotubes with the narrow-band-gap semiconductor nanoparticles CdS ^[156–158] and ZnS ^[159] by ion-exchange, followed by sulfidation with H_2S , have been reported. Such heterojunction photocatalysts show a moderate activity for dye oxidation, but the

photocorrosion of sulfides is a major problem in such systems. Sensitisation of titanate nanofibres with NiO nanoparticles^[160] or tin porphyrin (Sn-TTP) complexes intercalated between layers of titanates^[161] also resulted in photocatalytic activity of the composite material in the visible range of wavelengths. For the last case, femtosecond studies showed effective charge separation of visible light photoinduced carriers. The photocatalytic oxidation of methyl orange showed a synergistic enhancement of activity under both UV and visible illumination.^[161]

In conclusion, elongated titanate and TiO₂ nanostructures have been considered for photocatalytic processes including oxidation of organic waste in air and water,^[140,141,162] splitting of water^[155,163] and generation of hydrogen by using sacrificial hole scavengers^[146,164,165] (see Table 4). A comparison of elongated morphologies^[164] for hydrogen evolution from methanol indicated that the photocatalytic activity followed the trend: anatase NF > TiO₂-(B) NF >> H-TiNF. Systematic studies of all elongated morphologies including nanotubes, nanosheets and nanofibres transformed from each other by calcination or hydrothermal treatment are needed.

Glass surfaces coated with photocatalytically active TiO₂ are already commercially used as self-cleaning surfaces, which, under UV light, gain antifogging and super hydrophilic properties.^[3] Elongated H-TiNT and TiO₂ anatase nanorods^[166,167] demonstrate even better surface wettability, as the tubular morphology results in an increased surface roughness, which can be beneficial for achieving a smaller contact angle between the surface coating and the water droplet.

3.4. Solar Cells

Elongated titanates and TiO₂ nanostructures have also been examined as electrodes for dye-sensitised solar cells (DSSCs). Figure 8 a) shows the principle of a DSSC operating with nanotubular titanates. The photoexcited molecule of dye adsorbed on the surface of nanotubes injects an electron to the semiconductor, which diffuses towards the electron sink. The oxidised form of the dye is reduced by iodide ions in the electrolyte solution, and the released iodine is further reduced on the platinum counter electrode.

The potential advantage of titanate nanotubes as electrodes for DSSCs can be realised by utilising the phenomenon of better (relative to TiO₂ NP) adsorption of the positively charged dyes from aqueous solution on the surface of negatively charged titanate nanotubes,^[168] allowing a compact monolayer of dye to be deposited with a capacity of over 1000 molecules per nanotube. Such a dense loading of dye would allow the thickness of the light-absorbing layer of the electrode to be reduced from typical values of several microns to much lower values and decrease the electron diffusion distance, which would potentially improve the charge collection. The second advantage of nanotubes is their elongated morphology, which can provide a direct pathway for electron transfer from the point of injection to the electron

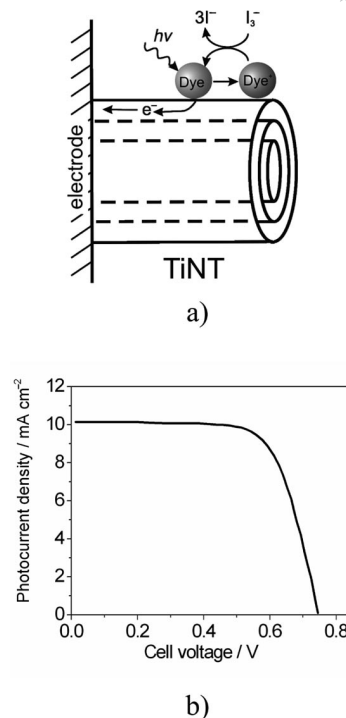


Figure 8. Applications of titanate nanotubes for a dye-sensitised solar cell: (a) the sketch of the processes in a DSSC, (b) photocurrent–voltage curve for a DSSC with a TiO₂ NR electrode (Adapted from ref.^[173]).

sink with an improved electron transport and a higher charge collection efficiency.

The design and manufacture of conventional DSSCs was optimised for a nanoparticulate TiO₂ electrode, which can withstand high-temperature calcination and is a more suitable adsorbent for negatively charged dye molecules [*cis*-bis(thiocyanato)bis(2,2-bipyridyl-4,4-di-carboxylato)ruthenium(II) complex]. In contrast, titanate nanotubes are more suitable for the adsorption of positively charged dyes and less stable during calcination at 450 °C,^[61–65] which is required for the conventional doctor blade method of electrode manufacture. For these reasons, early data showed that titanate nanotubes can be applied as electrodes in DSSCs; however, no significant benefit was observed relative to electrodes based on TiO₂ nanoparticles.^[169] In fact, in most of the studies, calcination of the electrode at 450 °C was used in order to remove the polyethylene glycol binder, meaning that TiO₂ anatase nanorods instead of H-TiNT were used in the DSSCs.

An alternative way to achieve immobilisation of elongated titanates is a direct alkaline hydrothermal synthesis of nanotubes on the surface of titanium metal.^[170,171] In this process, the sample was calcinated at 500 °C before dye incorporation, resulting in the conversion of H-TiNT to TiO₂ anatase NR.^[61–65] Thus, the advantage of increased dye adsorption on the surface of titanate nanotubes still has not been fully realised.

In order to benefit from the improvement of electron transport in elongated nanostructures, it is necessary to as-

semble nanostructures on the surface of the electrode. In most of the reports, elongated titanates are randomly oriented, diminishing the advantage of direct transport; however, a recent successful alignment of titanate nanofibres on the surface of titanium under alkaline hydrothermal synthesis at 180 °C resulted in an improved efficiency of the DSSC relative to that with P25 TiO₂.^[172]

Detailed studies of the electron relaxation kinetics in elongated TiO₂ anatase nanorods showed that the electron diffusion coefficient in nanorods is similar to that in P25; however, the electron lifetime is three times higher than that in P25, because of possible suppression of recombination between electrons and I⁻ ions on the surface of the nanorods,^[173] resulting in a higher value of the open circuit potential. Transient studies using intensity-modulated photocurrent spectroscopy showed the improvement of charge collection to be in the following order: P25, titanate nanotubes and anatase nanorods.^[174] The charge collection ratio, defined as a ratio of the recombination time constant to the electron collection time (τ_r/τ_c), was found to be ca. 150, 50 and 10 for TiO₂ NR, H-TiNT and P25, respectively. These results were obtained for randomly oriented nanotubes and nanorods. The improvement of the alignments of the nanotubes on the electrode would potentially further improve the electron collection efficiency.

Polycrystalline nanoparticles of anatase obtained from titanate nanotubes by hydrothermal treatment at 240 °C in the presence of dilute HNO₃ showed a slightly higher I_{sc} but a lower V_{oc} relative to P25 in the DSSC, which was probably due to the higher recombination rate of charge carriers in these nanoparticles.^[175]

The typical efficiency of a DSSC with elongated TiO₂ NR operating with a standard dye and electrolyte approaches 7.1%,^[173] and the voltammetric curve has the shape shown in Figure 8b. Another type of TiO₂ nanotube array, produced by anodising a Ti surface having a smaller specific surface area, also attracts attention as a prospective material for DSSC electrodes,^[176] since the ordered structures on the electrode allow an improved electron transfer, resulting in an efficiency of ca. 4.1%. The TiO₂ nanotubes obtained by template hydrolysis have also been studied in a DSSC, with a reported efficiency of ca. 8.4%.^[177]

Due to leakage problems associated with a liquid-electrolyte DSSC, attention has been paid recently to solid- or gel-electrolyte DSSCs. The addition of H-TiNT filler to a polyethylene glycol gel electrolyte up to a 10% content of nanotubes has facilitated improved ionic conductivity in the gel.^[178]

3.5. New Materials

3.5.1. Magnetic Materials

Recent interest in room-temperature ferromagnetic semiconductors and magnetic nanosized materials having a high aspect ratio (motivated by possible application in spin-base semiconductor devices) has stimulated research into the synthesis and characterisation of elongated titanates and

TiO₂ magnetic materials. Pure titanate nanotubes have paramagnetic properties;^[179] doping nanotubes with Co²⁺ results in ferromagnetic properties with a coercivity of ca. 40 Oe.^[180]

Several methods have been reported for doping titanate nanotubes with cobalt. The first is in situ doping, where addition of a cobalt(II) salt into a TiO₂/NaOH mixture, followed by alkaline hydrothermal treatment, results in the formation of titanate nanotubes.^[181] A similar method is the use of Co-doped TiO₂ as a feedstock for the preparation of nanotubes by an alkaline hydrothermal route.^[180] In both processes, crystallisation of titanate nanotubes results in the arrangement of Co^{II} ions at octahedral positions of Ti⁴⁺ in the titanate lattice.^[179] In this case, the room-temperature ferromagnetism is probably associated with oxygen vacancies resulting from such a substitution.^[182]

In contrast, according to ref.^[48] and our unpublished results, titanate nanotubes ion-exchanged with Co²⁺ having a Co/Ti ratio of 1:3.5 possess antiferromagnetic properties at room temperature, probably as a result of Co–Co interactions. It was shown, however, that, in case of titanate nanofibres ion-exchanged with Co²⁺, hydrothermal treatment of the sample at 160 °C in water results in substitution of titanium by cobalt and the appearance of ferromagnetic properties.^[183] The ferromagnetism decreased at higher Co^{II} levels, however, due to the superexchange coupling between cobalt ions in the lattice.

Calcination of Co-doped TiNT at 400 °C and 500 °C results in formation of Co-doped TiO₂-(B) NT and anatase NR, respectively. Both nanostructures are characterised by ferromagnetic properties, and the highest saturation magnetisation is observed in Co-TiO₂-(B) NT.^[181] Cobalt-doped TiNF can also be produced in situ by addition of Co^{II} to a TiO₂/NaOH mixture followed by alkaline hydrothermal treatment at temperatures higher than 170 °C. Calcination of such Co-TiNF structures at 700 °C results in their transformation to anatase nanofibres. Both nanofibre materials have ferromagnetic properties.^[117] Quantum calculations suggest that Fe^{III}-doped titanate nanotubes could possess magnetic insulator properties.^[184] Nickel nanoparticles deposited on the surface of TiNTs also show ferromagnetic properties.^[185]

3.5.2. Hydrogen Storage and Sensing

Hydrogen storage has become a hot topic in recent years because of the possibility of the broad implementation of hydrogen as a major energy carrier in the hydrogen economy. Currently, there are several commercially available technologies to store hydrogen, including physisorption of hydrogen on high-specific-surface-area materials at cryogenic temperatures or chemisorption of hydrogen onto nanoparticles of metal alloys by forming hydrides.^[186] In the first case, the interaction between hydrogen and adsorbent materials is relatively weak (ca. 10 kJ mol⁻¹).^[187] This necessitates the use of low temperatures or a high pressure of hydrogen to achieve high values of hydrogen uptake. In the case of chemisorption, the interaction between hydrogen and adsorbent materials is too strong (in the order of

magnitude of 100 kJ mol^{-1}),^[187] resulting in the need for high temperatures to release gaseous hydrogen.

As a result of these limitations in known hydrogen adsorption technologies, there is a current search for systems with a new type of interaction between the gas and the capturing material, which are characterised by intermediate values of interaction energy in the range $30\text{--}60 \text{ kJ mol}^{-1}$. Such an intermediate bond strength might facilitate a reversible sorption system, which can operate under near ambient conditions and provide a high degree of hydrogen uptake.

The ability of titanate nanotubes to reversibly accumulate molecular hydrogen with a relatively high uptake over a wide range of temperature from -196°C to 125°C ^[188,189] opens up the possibility of hydrogen storage and related applications. Early data showed that values of the enthalpy and the activation energy of hydrogen sorption into titanate nanotubes could be estimated as ca. -30 kJ mol^{-1} and 44 kJ mol^{-1} , respectively.^[188] The exact mechanism and the nature of bonded hydrogen are still under investigation. It has been suggested that hydrogen can occupy interstitial cavities between layers in the walls of the nanotubes without chemical bond formation. The OH groups in the nanotube lattice could stabilise the hydrogen molecules by weak van der Waals interactions, resulting in the formation of $\text{H-TiNT}\cdot x\text{H}_2$ clathrates, which might show similarities to the recently reported hydrogen clathrate hydrate $(32+x)\text{H}_2\cdot 136\text{H}_2\text{O}$.^[190]

An interesting property of TiO_2 nanotubes produced by anodising is that their electrical resistance decreases by several orders of magnitude in the presence of sufficient hydrogen.^[191] The titanate nanotubes^[192] and Pt- or Pd-decorated titanate nanotubes^[193] also possess a similar hydrogen sensing behaviour, allowing the manufacture of integrated systems, which can self-control the amount of intercalated hydrogen. Nanofibrous $\text{TiO}_2\text{-(B)}$ can also be used as a humidity sensor.^[194]

3.5.3. Composites, Surface Coatings and Tribology

Composite materials based on elongated nanostructures can bring additional functionality, structural reinforcement and potentially extend the number of applications of such materials. A few approaches to the manufacture of titanate nanotube polymer composites have been reported recently with use of polystyrene^[195] or polyurethane^[196] matrices. In both cases, the effective dispersion of TiNT has been achieved by hydrophobisation of the surface by using siloxanes or surface adsorption of hexamethylene diisocyanate prior to mixing with polystyrene and polyurethane, respectively. The films of TiNT/polystyrene composites were characterised by an increase in the Young modulus and tensile strength at even low loading levels of nanotubes.^[195] The comprehensive tribological studies of TiNT/polyurethane composites have revealed the significant improvement of the wear resistance and the decrease in the friction coefficient of composites relative to the pure polymer.^[196]

The prospective TiNT/polyaniline composites obtained by oxidation of aniline adsorbed on the surface of nanotu-

bes in the presence of triblock copolymers^[197] are interesting, because of the unusual combination of electroconductive and proton-conductive properties of the polymer and the nanotubes, respectively. Similar composites of TiNT with proton-conductive Nafion have also demonstrated advantages relative to the pure polymer.^[101] The long titanate nanofibres in aqueous suspensions with^[198] or without^[199] the addition of Pluronic (F127) surfactant may form a pulp, which can be cast into a free-standing (paper like) membrane. These membranes have an open pore structure with a pore size of ca. $0.05 \mu\text{m}$ and can be used as a filter or catalyst during the oxidation of organic wastes.

One of the practical questions is how to immobilise titanate nanotubes on the surface of the substrate for engineering applications. Many approaches to the manufacture of TiNT films have been used, including the doctor blade technique from the slurry mixture,^[104,169] electrophoretic deposition on the anode from aqueous electrolyte with addition of polycations as counterions,^[46,166] anodising of titanium in the presence of fluoride ions,^[11,10] in situ growth on the surface of titanium under alkaline hydrothermal synthesis^[170,171] spin coating,^[200] hot pressing of the TiNT powder,^[24] Langmuir-Blodgett deposition^[201] and layer-by-layer assembly.^[166,167] All of these methods can produce film composites, which are characterised by various thicknesses, densities, compositions of titanates and degrees of self-assembly.

Further developments in the synthesis and characterisation of novel composite films are likely to be an active area of future research. In particular, problems related to the self-assembly of elongated nanostructures are most challenging, since positive outcomes would allow significant improvements in the performance of existing and near-term devices such as dye-sensitised solar cells.

3.6. Biomedical Applications

Recently, the use of nanostructured inorganic materials in various biological applications, including controlled drug delivery, labelling of biological objects and building of artificial tissues from nanostructured composite materials has become an active area of research.^[202,203]

Because of their moderate electroconductivity, high surface area and affinity towards positively charged ions in aqueous solution, elongated nanostructured titanates have recently been studied as possible elements of amperometric biosensors. It has been shown that the redox mediator Meldola blue^[204] and such oxygen transport metalloproteins as haemoglobin^[205] or myoglobin^[206] can easily be immobilised on the surface of TiNT, providing an efficient electron transfer facility between biological molecules and an artificial electrode, which is usually a challenging task because of the poor compatibility between inorganic materials and biomolecules. Improved charge transfer in such systems can be utilised in biosensors, e.g. for glucose and NADH.

The studies of ibuprofen adsorption in the pores of TiNT have revealed that the melting temperature of ibuprofen is

decreased from 78 °C in the bulk to 66 °C, which is closer to physiological temperatures and might be utilised for controlled drug delivery following improvements in the technology.^[207]

Titanium surfaces coated with titanate nanofibres produced by the alkaline hydrothermal method can be used as bioscaffolds for cell cultures, providing enough rigidity and large macroporous structure suitable for cell growth and nutrition.^[208] The biocompatibility of fibrous sodium titanate deposited inside the pores of anodised TiO₂ nanotube arrays has been recently demonstrated by observation of the increased growth of hydroxyapatite (HAp) from a simulated body fluid.^[209] The ability to stimulate crystallisation of HAp on the surface of titanates can be related to their good ion-exchange properties.^[50] Therefore, surfaces coated with elongated titanates are potentially useful to enable well-adhering bioactive surface layers on Ti substrates for orthopaedic and dental implants.

Further developments of elongated titanates as materials for biotechnology would require comprehensive studies of their cytotoxicity. Improvement in the methods of filling nanotube pores with bioactive drug molecules would provide a significant step towards the development of controlled drug delivery systems.

3.7. Other Applications

There is a range of recently emerged studies suggesting possible applications of elongated titanates and TiO₂ in areas that are not intrinsic to TiO₂ materials. Examples include the use of high-surface-area elongated titanates as low-cost adsorbents for chromatography^[47,210] and for dye removal from wastes of stained fabrics in the textile industry.^[168]

The high surface area and the acidic nature of nanotubular titanate surfaces also render these materials useful as a coating for quartz crystal microbalance devices. For example, various amines have been detected in the gas phase, which is relevant to the monitoring of chemical warfare agents.^[211]

The high aspect ratio of elongated titanates can also be utilised in liquid suspensions, namely nanofluids, which are characterised by unusual electrorheological^[212] and thermoconductive^[213] properties. Such fluids can be used in the active control of conventional and intelligent devices in which viscosity or thermoconductivity is modulated by an applied electric field.

4. Conclusions

Recently, nanostructured materials of elongated titanates and TiO₂ produced by the alkaline hydrothermal method have been shown to possess unique combinations of morphological and physicochemical properties leading to a variety of possible applications. Among the useful physicochemical properties of titanate nanotubes and nanofibres are a high specific surface area, a mesoporous range of pore

sizes, efficient ion-exchange, electroconductivity and ionic conductivity. The low cost and simplicity of manufacture and facile control of the morphology of elongated titanates could stimulate their mass production, provided that there is sufficient demand. The demand for such materials could be driven by the future growth of renewable energy technologies, including solar and fuel cells, lithium batteries and hydrogen storage devices in which elongated titanates and TiO₂ have already demonstrated significant promise.

Future growth of research interest in elongated titanates is also anticipated in the areas of (1) preparation and tribological characterisation of composite multifunction smart coating, (2) biomedical applications including biosensors, biocompatible coatings and nanotubular drug delivery systems and (3) environmental applications including wastewater treatment and heavy metal recovery. The versatile chemistry of nanotubular titanates, together with the recent discovery of mutual transformations between elongated titanates and TiO₂, open a new low-cost route for the synthesis of novel materials.

Important challenges for the further development of elongated titanate nanostructures include: (1) improved knowledge of the relationship between synthesis conditions and the morphology of nanostructures, (2) compilation of a database describing structure–property relationships in titanate nanostructures and (3) improved knowledge of the mechanism of formation of elongated nanostructures, which will allow tailored nanostructures to be realised by adequate control of the synthesis route and process conditions. Both experimental design and mathematical modeling approaches will need to be used in an integrated fashion.

Acknowledgments

The authors gratefully acknowledge financial support from the Environmental and Physical Sciences Research Council (EPSRC) through UK grant EP/F044445/1, “A hydrothermal route to metal oxide nanotubes: synthesis and energy conversion application”.

- [1] R. I. Jaffee, N. E. Promisel (Eds.), *The Science, Technology, and Application of Titanium: Proceedings of the International Conference on Titanium (1st: 1968: London)*, Pergamon Press, Oxford, New York, **1970**.
- [2] A. Fujishima, K. Honda, *Nature* **1972**, 238, 37–38.
- [3] A. Fujishima, K. Hashimoto, T. Watanabe, *TiO₂ Photocatalysis: Fundamentals and Applications*, BKC, USA, **1999**.
- [4] T. Kasuga, M. Hiramatsu, A. Hoson, T. Sekino, K. Niihara, *Langmuir* **1998**, 14, 3160–3163.
- [5] S. Iijima, *Nature* **1991**, 354, 56–58.
- [6] X. Chen, S. S. Mao, *Chem. Rev.* **2007**, 107, 2891–2959.
- [7] D. V. Bavykin, J. M. Friedrich, F. C. Walsh, *Adv. Mater.* **2006**, 18, 2807–2824.
- [8] Q. Chen, L.-M. Peng, *Int. J. Nanotechnol.* **2007**, 4, 44–65.
- [9] H. H. Ou, S. L. Lo, *Sep. Purif. Technol.* **2007**, 58, 179–191.
- [10] C. A. Grimes, *J. Mater. Chem.* **2007**, 17, 1451–1457.
- [11] G. K. Mor, O. K. Varghese, M. Paulose, K. Shankar, C. A. Grimes, *Sol. Energy Mater. Sol. Cells* **2006**, 90, 2011–2075.
- [12] J. M. Macak, H. Tsuchiya, A. Ghicov, K. Yasuda, R. Hahn, S. Bauer, P. Schmuki, *Curr. Opin. Solid State Mater. Sci.* **2007**, 11, 3–18.

- [13] C. Bae, H. Yoo, S. Kim, K. Lee, J. Kim, M. M. Sung, H. Shin, *Chem. Mater.* **2008**, *20*, 756–767.
- [14] N. Viriyaempikul, N. Sano, T. Charinpanitkul, T. Kikuchi, W. Tanthapanichakoon, *Nanotechnology* **2008**, *19*, 035601–6.
- [15] A. Kukovecz, M. Hodos, E. Horvath, G. Radnoczi, Z. Konya, I. Kiricsi, *J. Phys. Chem. B* **2005**, *109*, 17781–17783.
- [16] D. V. Bavykin, V. N. Parmon, A. A. Lapkin, F. C. Walsh, *J. Mater. Chem.* **2004**, *14*, 3370–3377.
- [17] Y. Mao, M. Kanungo, T. Hemraj-Benny, S. S. Wong, *J. Phys. Chem. B* **2006**, *110*, 702–710.
- [18] Y. Wang, J. Yang, J. Zhang, H. Liu, Z. Zhang, *Chem. Lett.* **2005**, *34*, 1168–1169.
- [19] H. H. Ou, S. L. Lo, Y. H. Liou, *Nanotechnology* **2007**, *18*, 175702–6.
- [20] X. Wu, Q. Z. Jiang, Z. F. Ma, M. Fu, W. F. Shangguan, *Solid State Commun.* **2005**, *136*, 513–517.
- [21] X. Wu, Q. Z. Jiang, Z. F. Ma, W. F. Shangguan, *Solid State Commun.* **2007**, *143*, 343–347.
- [22] Y. Ma, Y. Lin, X. Xiao, X. Zhou, X. Li, *Mater. Res. Bull.* **2006**, *41*, 237–243.
- [23] E. Horvath, A. A. Kukovecz, Z. Konya, I. Kiricsi, *Chem. Mater.* **2007**, *19*, 927–931.
- [24] T. Kubo, A. Nakahira, Y. Yamasaki, *J. Mater. Res.* **2007**, *22*, 1286–1291.
- [25] M. Wei, Y. Konishi, H. Arakawa, *J. Mater. Sci.* **2007**, *42*, 529–533.
- [26] J. J. Yang, Z. S. Jin, X. D. Wang, W. Li, J. W. Zhang, S. L. Zhang, X. Y. Guo, Z. J. Zhang, *Dalton Trans.* **2003**, *20*, 3898–3901.
- [27] R. Ma, Y. Bando, T. Sasaki, *J. Phys. Chem. B* **2004**, *108*, 2115–2119.
- [28] N. Sakai, Y. Ebina, K. Takada, T. Sasaki, *J. Am. Chem. Soc.* **2004**, *126*, 5851–5858.
- [29] D. V. Bavykin, B. A. Cressey, M. E. Light, F. C. Walsh, *Nanotechnology* **2008**, *19*, 275604–5.
- [30] Z. Y. Yuan, B. L. Su, *Colloids Surf. A* **2004**, *241*, 173–183.
- [31] G. H. Du, Q. Chen, P. D. Han, Y. Yu, L. M. Peng, *Phys. Rev. B* **2003**, *67*, 035323–7.
- [32] X. Sun, X. Chen, Y. Li, *Inorg. Chem.* **2002**, *41*, 4996–4998.
- [33] B. Wang, Y. Shi, D. Xue, *J. Solid State Chem.* **2007**, *180*, 1028–1037.
- [34] D. V. Bavykin, B. A. Cressey, F. C. Walsh, *Aust. J. Chem.* **2007**, *60*, 95–98.
- [35] W. A. Daoud, G. K. H. Pang, *J. Phys. Chem. B* **2006**, *110*, 25746–25750.
- [36] G. H. Du, Q. Chen, R. C. Che, Z. Y. Yuan, L. M. Peng, *Appl. Phys. Lett.* **2001**, *79*, 3702–3704.
- [37] Q. Chen, G. H. Du, S. Zhang, L. M. Peng, *Acta Crystallogr. Sect. B: Struct. Sci.* **2002**, *58*, 587–593.
- [38] A. Nakahira, W. Kato, M. Tamai, T. Isshiki, K. Nishio, H. Aritani, *J. Mater. Sci.* **2004**, *39*, 4239–4245.
- [39] R. Z. Ma, Y. Bando, T. Sasaki, *Chem. Phys. Lett.* **2003**, *380*, 577–582.
- [40] R. Z. Ma, K. Fukuda, T. Sasaki, M. Osada, Y. Bando, *J. Phys. Chem. B* **2005**, *109*, 6210–6224.
- [41] G. Armstrong, A. R. Armstrong, J. Canales, P. G. Bruce, *Chem. Commun.* **2005**, *19*, 2454–2456.
- [42] B. Poudel, W. Z. Wang, C. Dames, J. Y. Huang, S. Kunwar, D. Z. Wang, D. Banerjee, G. Chen, Z. F. Ren, *Nanotechnology* **2005**, *16*, 1935–1940.
- [43] S. K. Pradhan, Y. Mao, S. S. Wong, P. Chupas, V. Petkov, *Chem. Mater.* **2007**, *19*, 6180–6186.
- [44] Z. V. Saponjic, N. M. Dimitrijevic, D. M. Tiede, A. J. Goshe, X. Zuo, L. X. Chen, A. S. Barnard, P. Zapol, L. Curtiss, T. Rajh, *Adv. Mater.* **2005**, *17*, 965–971.
- [45] T. Kubo, A. Nakahira, *J. Phys. Chem. C* **2008**, *112*, 1658–1662.
- [46] J. Yu, M. Zhou, *Nanotechnology* **2008**, *19*, 045606–045612.
- [47] H. Niu, Y. Cai, Y. Shi, F. Wei, S. Mou, G. Jiang, *J. Chromatogr. A* **2007**, *1172*, 113–120.
- [48] X. Sun, Y. Li, *Chem. Eur. J.* **2003**, *9*, 2229–2238.
- [49] E. Morgado, M. A. S. de Abreu, G. T. Moure, B. A. Marinkovic, P. M. Jardim, A. S. Araujo, *Chem. Mater.* **2007**, *19*, 665–676.
- [50] D. V. Bavykin, F. C. Walsh, *J. Phys. Chem. C* **2007**, *111*, 14644–14651.
- [51] M. Wei, Y. Konishi, H. Zhou, H. Sugihara, H. Arakawa, *Solid State Commun.* **2005**, *133*, 493–498.
- [52] C. C. Tsai, H. Teng, *Langmuir* **2008**, *24*, 3434–3438.
- [53] G. Mogilevsky, Q. Chen, H. Kulkarni, A. Kleinhammes, W. M. Mullins, Y. Wu, *J. Phys. Chem. C* **2008**, *112*, 3239–3246.
- [54] A. Vittadini, M. Casarin, *Theor. Chem. Account.* **2008**, *120*, 551–556.
- [55] A. Vittadini, M. Casarin, A. Selloni, *Theor. Chem. Account* **2007**, *117*, 663–671.
- [56] F. Alvarez-Ramirez, Y. Ruiz-Morales, *Chem. Mater.* **2007**, *19*, 2947–2959.
- [57] S. Zhang, L. M. Peng, Q. Chen, G. H. Du, G. Dawson, W. Z. Zhou, *Phys. Rev. Lett.* **2003**, *91*, 256103–256107.
- [58] S. Zhang, Q. Chen, L. M. Peng, *Phys. Rev. B* **2005**, *71*, 014104–014115.
- [59] A. Thorne, A. Kruth, D. Tunstall, J. T. S. Irvine, W. Zhou, *J. Phys. Chem. B* **2005**, *109*, 5439–5444.
- [60] C. C. Chung, T. W. Chung, T. C. K. Yang, *Ind. Eng. Chem. Res.* **2008**, *47*, 2301–2307.
- [61] E. Morgado Jr, P. M. Jardim, B. A. Marinkovic, F. C. Rizzo, M. A. S. Abreu, J. L. Zotin, A. S. Araujo, *Nanotechnology* **2007**, *18*, 495710.
- [62] M. Qamar, C. R. Yoon, H. J. Oh, D. H. Kim, J. H. Jho, K. S. Lee, W. J. Lee, H. G. Lee, S. J. Kim, *Nanotechnology* **2006**, *17*, 5922–5929.
- [63] E. Morgado Jr, M. A. S. Abreu, O. R. C. Pravia, B. A. Marinkovic, P. M. Jardim, F. C. Rizzo, A. S. Araujo, *Solid State Sci.* **2006**, *8*, 888–900.
- [64] E. Morgado Jr, M. A. S. Abreu, G. T. Moure, B. A. Marinkovic, P. M. Jardim, A. S. Araujo, *Mater. Res. Bull.* **2007**, *42*, 1748–1760.
- [65] C. K. Lee, C. C. Wang, M. D. Lyu, L. C. Juang, S. S. Liu, S. H. Hung, *J. Colloid Interface Sci.* **2007**, *316*, 562–569.
- [66] O. P. Ferreira, A. G. Souza-Filho, J. Mendes-Filho, O. L. Alves, *J. Braz. Chem. Soc.* **2006**, *17*, 393–402.
- [67] S. Pavasupree, Y. Suzuki, S. Yoshikawa, R. Kawahata, *J. Solid State Chem.* **2005**, *178*, 3110–3116.
- [68] R. Yoshida, Y. Suzuki, S. Yoshikawa, *J. Solid State Chem.* **2005**, *178*, 2179–2185.
- [69] H. Yu, J. Yu, B. Cheng, M. Zhou, *J. Solid State Chem.* **2006**, *179*, 349–354.
- [70] Y. V. Kolen'ko, K. A. Kovnir, A. I. Gavrillov, A. V. Garshev, J. Frantti, O. I. Lebedev, B. R. Churagulov, G. V. Tendeloo, M. Yoshimura, *J. Phys. Chem. B* **2006**, *110*, 4030–4038.
- [71] H. Y. Zhu, Y. Lan, X. P. Gao, S. P. Ringer, Z. F. Zheng, D. Y. Song, J. C. Zhao, *J. Am. Chem. Soc.* **2005**, *127*, 6730–6736.
- [72] J. N. Nian, H. Teng, *J. Phys. Chem. B* **2006**, *110*, 4193–4198.
- [73] D. V. Bavykin, J. M. Friedrich, A. A. Lapkin, F. C. Walsh, *Chem. Mater.* **2006**, *18*, 1124–1129.
- [74] Y. Mao, S. S. Wong, *J. Am. Chem. Soc.* **2006**, *128*, 8217–8226.
- [75] N. Wang, H. Lin, J. Li, L. Zhang, C. Lin, X. Li, *J. Am. Ceram. Soc.* **2006**, *89*, 3564–3566.
- [76] T. Gao, Q. Wu, H. Fjellvag, P. Norby, *J. Phys. Chem. C* **2008**, *112*, 8548–8552.
- [77] C. H. Lin, S. H. Chien, J. H. Chao, C. Y. Sheu, Y. C. Cheng, Y. J. Huang, C. H. Tsai, *Catal. Lett.* **2002**, *80*, 153–159.
- [78] A. Kleinhammes, G. W. Wagner, H. Kulkarni, Y. Jia, Q. Zhang, L. C. Qin, Y. Wu, *Chem. Phys. Lett.* **2005**, *411*, 81–85.
- [79] D. V. Bavykin, A. A. Lapkin, P. K. Plucinski, L. Torrente-Murciano, J. M. Friedrich, F. C. Walsh, *Top. Catal.* **2006**, *39*, 151–160.
- [80] F. C. Walsh, D. V. Bavykin, L. Torrente-Murciano, A. A. Lapkin, B. A. Cressey, *Trans. Inst. Met. Finish.* **2006**, *84*, 293–299.
- [81] B. Zhu, Q. Guo, X. Huang, S. Wang, S. Zhang, S. Wu, W. Huang, *J. Mol. Catal. A* **2006**, *249*, 211–217.

- [82] B. Zhu, Q. Guo, S. Wang, X. Zheng, S. Zhang, S. Wu, W. Huang, *React. Kinet. Catal. Lett.* **2006**, *88*, 301–308.
- [83] J. Jiang, Q. Gao, Z. Chen, *J. Mol. Catal. A* **2008**, *280*, 233–239.
- [84] B. Zhu, K. Li, Y. Feng, S. Zhang, S. Wu, W. Huang, *Catal. Lett.* **2007**, *118*, 55–58.
- [85] B. Zhu, X. Zhang, S. Wang, S. Zhang, S. Wu, W. Huang, *Microporous Mesoporous Mater.* **2007**, *102*, 333–336.
- [86] S. H. Chien, Y. C. Liou, M. C. Kuo, *Synth. Met.* **2005**, *152*, 333–336.
- [87] V. Idakiev, Z. Y. Yuan, T. Tabakova, B. L. Su, *Appl. Catal. A* **2005**, *281*, 149–155.
- [88] L. M. Sikhivihilu, N. J. Coville, D. Naresh, K. V. R. Chary, V. Vishwanathan, *Appl. Catal. A* **2007**, *324*, 52–61.
- [89] L. M. Sikhivihilu, N. J. Coville, B. M. Pulimaddi, J. Venkatreddy, V. Vishwanathan, *Catal. Commun.* **2007**, *8*, 1999–2006.
- [90] L. Torrente-Murciano, A. A. Lapkin, D. V. Bavykin, F. C. Walsh, K. Wilson, *J. Catal.* **2007**, *245*, 270–276.
- [91] J. N. Nian, S. A. Chen, C. C. Tsai, H. Teng, *J. Phys. Chem. B* **2006**, *110*, 25817–25824.
- [92] D. V. Bavykin, A. A. Lapkin, P. K. Plucinski, J. M. Friedrich, F. C. Walsh, *J. Catal.* **2005**, *235*, 10–17.
- [93] M. A. Cortes-Jacome, M. Morales, C. Angeles-Chavez, L. F. Ramirez-Verduzco, E. Lopez-Salinas, J. A. Toledo-Antonio, *Chem. Mater.* **2007**, *19*, 6605–6614.
- [94] M. A. Cortes-Jacome, C. Angeles-Chavez, M. Morales, E. Lopez-Salinas, J. A. Toledo-Antonio, *J. Solid State Chem.* **2007**, *180*, 2682–2689.
- [95] C. Hippe, M. Wark, E. Lork, G. Schulz-Ekloff, *Microporous Mesoporous Mater.* **1999**, *31*, 235–239.
- [96] Y. Sato, M. Koizumi, T. Miyao, S. Naito, *Catal. Today* **2006**, *111*, 164–170.
- [97] M. Wang, D. J. Guo, H. L. Li, *J. Solid State Chem.* **2005**, *178*, 1996–2000.
- [98] F. Hu, F. Ding, S. Song, P. K. Shen, *J. Power Sources* **2006**, *163*, 415–419.
- [99] H. Song, X. Qiu, D. Guo, F. Li, *J. Power Sources* **2008**, *178*, 97–102.
- [100] C. Ponce-de-Leon, D. V. Bavykin, F. C. Walsh, *Electrochem. Commun.* **2006**, *8*, 1655–1660.
- [101] B. R. Matos, E. I. Santiago, F. C. Fonseca, M. Linardi, V. Lavayen, R. G. Lacerda, L. O. Ladeira, A. S. Ferlauto, *J. Electrochem. Soc.* **2007**, *154*, B1358–B1361.
- [102] F. Cheng, Z. Tao, J. Liang, J. Chen, *Chem. Mater.* **2008**, *20*, 667–681.
- [103] F. Cheng, J. Chena, *J. Mater. Res.* **2006**, *21*, 2744–2757.
- [104] J. Li, Z. Tang, Z. Zhang, *Electrochem. Commun.* **2005**, *7*, 62–67.
- [105] J. Li, Z. Tang, Z. Zhang, *Chem. Phys. Lett.* **2006**, *418*, 506–510.
- [106] Y. K. Zhou, L. Cao, F. B. Zhang, B. L. He, H. L. Liz, *J. Electrochem. Soc.* **2003**, *150*, A1246–A1249.
- [107] J. Li, Z. Tang, Z. Zhang, *Chem. Mater.* **2005**, *17*, 5848–5855.
- [108] X. Gao, H. Zhu, G. Pan, S. Ye, Y. Lan, F. Wu, D. Song, *J. Phys. Chem. B* **2004**, *108*, 2868–2872.
- [109] L. Kavan, M. Kalbac, M. Zukalova, I. Exnar, V. Lorenzen, R. Nesper, M. Graetzel, *Chem. Mater.* **2004**, *16*, 477–485.
- [110] Q. Wang, Z. Wen, J. Li, *Inorg. Chem.* **2006**, *45*, 6944–6949.
- [111] H. Zhang, G. R. Li, L. P. An, T. Y. Yan, X. P. Gao, H. Y. Zhu, *J. Phys. Chem. C* **2007**, *111*, 6143–6148.
- [112] A. R. Armstrong, G. Armstrong, J. Canales, P. G. Bruce, *Adv. Mater.* **2005**, *17*, 862–865.
- [113] M. Zukalova, M. Kalbac, L. Kavan, I. Exnar, M. Graetzel, *Chem. Mater.* **2005**, *17*, 1248–1255.
- [114] A. R. Armstrong, G. Armstrong, J. Canales, P. G. Bruce, *J. Power Sources* **2005**, *146*, 501–506.
- [115] J. Xu, C. Jia, B. Cao, W. F. Zhang, *Electrochim. Acta* **2007**, *52*, 8044–8047.
- [116] J. Xu, Y. Wang, Z. Li, W. F. Zhang, *J. Power Sources* **2008**, *175*, 903–908.
- [117] X. W. Wang, X. P. Gao, G. R. Li, T. Y. Yan, H. Y. Zhu, *J. Phys. Chem. C* **2008**, *112*, 5384–5389.
- [118] L. P. An, X. P. Gao, G. R. Li, T. Y. Yan, H. Y. Zhu, P. W. Shen, *Electrochim. Acta* **2008**, *53*, 4573–4579.
- [119] B. L. He, B. Dong, H. L. Li, *Electrochem. Commun.* **2007**, *9*, 425–430.
- [120] Z. W. Zhao, Z. P. Guo, D. Wexler, Z. F. Ma, X. Wu, H. K. Liu, *Electrochem. Commun.* **2007**, *9*, 697–702.
- [121] J. Kim, J. Cho, *J. Electrochem. Soc.* **2007**, *154*, A542–A546.
- [122] J. Qu, X. Zhang, Y. Wang, C. Xie, *Electrochim. Acta* **2005**, *50*, 3576–3580.
- [123] B. Dong, B. L. He, J. Huang, G. Y. Gao, Z. Yang, H. L. Li, *J. Power Sources* **2008**, *175*, 266–271.
- [124] L. Yu, X. Zhang, *Mater. Chem. Phys.* **2004**, *87*, 168–172.
- [125] Y. G. Wang, Z. D. Wang, Y. Y. Xia, *Electrochim. Acta* **2005**, *50*, 5641–5646.
- [126] Y. G. Wang, X. G. Zhang, *Electrochim. Acta* **2004**, *49*, 1957–1962.
- [127] G. Bo, Z. Xiaogang, Y. Changzhou, L. Juan, Y. Long, *Electrochim. Acta* **2006**, *52*, 1028–1032.
- [128] F. Tao, Y. Shen, Y. Liang, H. Li, *J. Solid State Electrochem.* **2007**, *11*, 853–858.
- [129] H. K. Xin, Z. Xiaogang, L. Juan, *Electrochim. Acta* **2006**, *51*, 1289–1292.
- [130] A. Riss, T. Berger, H. Grothe, J. Bernardi, O. Diwald, E. Knoltinger, *Nano Lett.* **2007**, *7*, 433–438.
- [131] D. V. Bavykin, S. N. Gordeev, A. V. Moskalenko, A. A. Lapkin, F. C. Walsh, *J. Phys. Chem. B* **2005**, *109*, 8565–8569.
- [132] N. Sakai, Y. Ebina, K. Takada, T. Sasaki, *J. Am. Chem. Soc.* **2004**, *126*, 5851–5858.
- [133] L. Qian, Z. S. Jin, S. Y. Yang, Z. L. Du, X. R. Xu, *Chem. Mater.* **2005**, *17*, 5334–5338.
- [134] Q. Li, J. Zhang, Z. Jin, D. Yang, X. Wang, J. Yang, Z. Zhang, *Electrochem. Commun.* **2006**, *8*, 741–746.
- [135] T. Tachikawa, S. Tojo, M. Fujitsuka, T. Sekino, T. Majima, *J. Phys. Chem. B* **2006**, *110*, 14055–14059.
- [136] M. Qamar, C. R. Yoon, H. J. Oh, N. H. Lee, K. Park, D. H. Kim, K. S. Lee, W. J. Lee, S. J. Kim, *Catal. Today* **2008**, *131*, 3–14.
- [137] C. K. Lee, C. C. Wang, M. D. Lyu, L. C. Juang, S. S. Liu, S. H. Hung, *J. Colloid Interface Sci.* **2007**, *316*, 562–569.
- [138] H. H. Ou, C. H. Liao, Y. H. Liou, J. H. Hong, S. L. Lo, *Environ. Sci. Technol.* **2008**, *42*, 4507–4512.
- [139] G. S. Guo, C. N. He, Z. H. Wang, F. B. Gu, D. M. Han, *Talanta* **2007**, *72*, 1687–1692.
- [140] M. Zhang, Z. Jin, J. Zhang, X. Guo, J. Yang, W. Li, X. Wang, Z. Zhang, *J. Mol. Catal. A* **2004**, *217*, 203–210.
- [141] J. Yu, H. Yu, B. Cheng, C. Trapalis, *J. Mol. Catal. A* **2006**, *249*, 135–142.
- [142] Z. Gao, S. Yang, C. Sun, J. Hong, *Sep. Purif. Technol.* **2007**, *58*, 24–31.
- [143] J. Yu, H. Yu, B. Cheng, X. Zhao, Q. Zhang, *J. Photochem. Photobiol. A: Chem.* **2006**, *182*, 121–127.
- [144] Y. Yu, D. Xu, *Appl. Catal. B* **2007**, *73*, 166–171.
- [145] G. Li, S. Ciston, Z. V. Saponjic, L. Chen, N. M. Dimitrijevic, T. Rajh, K. A. Gray, *J. Catal.* **2008**, *253*, 105–110.
- [146] H. L. Kuo, C. Y. Kuo, C. H. Liu, J. H. Chao, C. H. Lina, *Catal. Lett.* **2007**, *113*, 1–2, 7–12.
- [147] H. Yu, J. Yu, B. Cheng, *J. Mol. Catal. A* **2006**, *253*, 99–106.
- [148] H. Yu, J. Yu, B. Cheng, J. Lin, *J. Hazard. Mater.* **2007**, *147*, 581–587.
- [149] H. Tokudome, M. Miyauchi, *Chem. Lett.* **2004**, *33*, 1108–1109.
- [150] H. Langhuan, S. Zhongxin, L. Yingliang, *J. Ceram. Soc. Jpn.* **2007**, *115*, 28–31.
- [151] Y. Chen, S. Zhang, Y. Yu, H. Wu, S. Wang, B. Zhu, W. Huang, S. Wu, *J. Dispersion Sci. Technol.* **2008**, *29*, 245–249.
- [152] C. Feng, Y. Wang, Z. Jin, J. Zhang, S. Zhang, Z. Wu, Z. Zhang, *New J. Chem.* **2008**, *32*, 1038–1047.

- [153] H. Yamashita, Y. Ichihashi, M. Takeuchi, S. Kishiguchi, M. Anpo, *J. Synchrotron Radiat.* **1999**, *6*, 451–452.
- [154] S. Zhang, Y. Chen, Y. Yu, H. Wu, S. Wang, B. Zhu, W. Huang, S. Wu, *J. Nanopart. Res.* **2008**, *10*, 871–875.
- [155] C. C. Tsai, H. Teng, *Appl. Surf. Sci.* **2008**, *254*, 4912–4918.
- [156] M. Hodos, E. Horvath, H. Haspel, A. Kukovecz, Z. Konya, I. Kiricsi, *Chem. Phys. Lett.* **2004**, *399*, 512–515.
- [157] M. W. Xiao, L. S. Wang, Y. D. Wu, X. J. Huang, Z. Dang, *Nanotechnology* **2008**, *19*, 015706–7.
- [158] J. Zhu, D. Yang, J. Geng, D. Chen, Z. Jiang, *J. Nanopart. Res.* **2008**, *10*, 729–736.
- [159] H. Li, B. Zhu, Y. Feng, S. Wang, S. Zhang, W. Huang, *J. Solid State Chem.* **2007**, *180*, 2136–2142.
- [160] H. Song, H. Jiang, T. Liu, X. Liu, G. Meng, *Mater. Res. Bull.* **2007**, *42*, 334–344.
- [161] J. H. Jang, K. S. Jeon, S. Oh, H. J. Kim, T. Asahi, H. Masuhara, M. Yoon, *Chem. Mater.* **2007**, *19*, 1984–1991.
- [162] H. Zhou, T. J. Park, S. S. Wong, *J. Mater. Res.* **2006**, *21*, 2941–2947.
- [163] M. Kitano, R. Mitsui, D. Rakhmawaty, E. Zeinhom, M. A. El-Bahy, M. Matsuoka, M. Ueshima, M. Anpo, *Catal. Lett.* **2007**, *119*, 217–221.
- [164] J. Jitputti, Y. Suzuki, S. Yoshikawa, *Catal. Commun.* **2008**, *9*, 1265–1271.
- [165] C. H. Lin, C. H. Lee, J. H. Chao, C. Y. Kuo, Y. C. Cheng, W. N. Huang, H. W. Chang, Y. M. Huang, M. K. Shih, *Catal. Lett.* **2004**, *98*, 61–66.
- [166] M. Miyauchi, H. Tokudome, *Thin Solid Films* **2006**, *515*, 2091–2096.
- [167] M. Miyauchi, H. Tokudome, *J. Mater. Chem.* **2007**, *17*, 2095–2100.
- [168] C. K. Lee, C. C. Wang, L. C. Juang, M. D. Lyu, S. H. Hung, S. S. Liu, *Colloids. Surf. A* **2008**, *317*, 164–173.
- [169] S. Uchida, R. Chiba, M. Tomiha, N. Masaki, M. Shirai, *Electrochem.* **2002**, *70*, 418–420.
- [170] J. E. Boercker, E. Enache-Pommer, E. S. Aydil, *Nanotechnology* **2008**, *19*, 095604–10.
- [171] M. Wei, Y. Konishi, H. Zhou, H. Sugihara, H. Arakawa, *J. Electrochem. Soc.* **2006**, *153*, A1232–A1236.
- [172] W. Wang, H. Lin, J. Li, N. Wang, *J. Am. Ceram. Soc.* **2008**, *91*, 628–631.
- [173] Y. Ohsaki, N. Masaki, T. Kitamura, Y. Wada, T. Okamoto, T. Sekino, K. Niihara, S. Yanagida, *Phys. Chem. Chem. Phys.* **2005**, *7*, 4157–4163.
- [174] E. Enache-Pommer, J. E. Boercker, E. S. Aydil, *Appl. Phys. Lett.* **2007**, *91*, 123116–3.
- [175] P. T. Hsiao, K. P. Wang, C. W. Cheng, H. Teng, *J. Photochem. Photobiol. A: Chem.* **2007**, *188*, 19–24.
- [176] K. Shankar, J. Bandara, M. Paulose, H. Wietasch, O. K. Varghese, G. K. Mor, T. J. LaTempa, M. Thelakkat, C. A. Grimes, *Nano Lett.* **2008**, *8*, 1654–1659.
- [177] S. Ngamsinlapasathian, S. Sakulkaemaruehai, S. Pavasupree, A. Kitiyanan, T. Sreethawong, Y. Suzuki, S. Yoshikawa, *J. Photochem. Photobiol. A: Chem.* **2004**, *164*, 145–151.
- [178] M. S. Akhtar, J. M. Chun, O. B. Yang, *Electrochem. Commun.* **2007**, *9*, 2833–2837.
- [179] C. Huang, X. Liu, L. Kong, W. Lan, Q. Su, Y. Wang, *Appl. Phys. A* **2007**, *87*, 781–786.
- [180] D. Wu, Y. Chen, J. Liu, X. Zhao, A. Li, N. Ming, *Appl. Phys. Lett.* **2005**, *87*, 112501–3.
- [181] X. W. Wang, X. P. Gao, G. R. Li, L. Gao, T. Y. Yan, H. Y. Zhu, *Appl. Phys. Lett.* **2007**, *91*, 143102–3.
- [182] S. V. Chong, K. Kadowaki, J. Xia, H. Idriss, *Appl. Phys. Lett.* **2008**, *92*, 232502–3.
- [183] H. Zhang, T. Ji, Y. Liu, J. Cai, *J. Phys. Chem. C* **2008**, *112*, 8604–8608.
- [184] X. G. Xu, X. Ding, Q. Chen, L. M. Peng, *Phys. Rev. B* **2006**, *73*, 165403–5.
- [185] J. Jiang, Q. Gao, Z. Chen, J. Hu, C. Wu, *Mater. Lett.* **2006**, *60*, 3803–3808.
- [186] L. Schlapbach, A. Züttel, *Nature* **2001**, *414*, 353–358.
- [187] A. Züttel, A. Borgschulte, L. Schlapbach, *Hydrogen as a Future Energy Carrier*, WILEY-VCH, Weinheim, **2008**.
- [188] D. V. Bavykin, A. A. Lapkin, P. K. Plucinski, J. M. Friedrich, F. C. Walsh, *J. Phys. Chem. B* **2005**, *109*, 19422–19427.
- [189] S. H. Lim, J. Luo, Z. Zhong, W. Ji, J. Lin, *Inorg. Chem.* **2005**, *44*, 4124–4126.
- [190] K. A. Lokshin, Y. Zhao, D. He, W. L. Mao, H. K. Mao, R. J. Hemley, M. V. Lobanov, M. Greenblatt, *Phys. Rev. Lett.* **2004**, *93*, 125503–2.
- [191] O. K. Vardhese, D. Gong, M. Paulose, K. O. Ong, E. C. Dickey, C. A. Grimes, *Adv. Mater.* **2003**, *15*, 624–627.
- [192] H. S. Kim, W. T. Moon, Y. K. Jun, S. H. Hong, *Sens. Actuators, B* **2006**, *120*, 63–68.
- [193] C. H. Han, D. W. Hong, I. J. Kim, J. Gwak, S. D. Han, K. C. Singh, *Sens. Actuators, B* **2007**, *128*, 320–325.
- [194] G. Wang, Q. Wang, W. Lu, J. Li, *J. Phys. Chem. B* **2006**, *110*, 22029–22034.
- [195] M. T. Byrne, J. E. McCarthy, M. Bent, R. Blake, Y. K. Gun'ko, E. Horvath, Z. Konya, A. Kukovecz, I. Kiricsi, J. N. Coleman, *J. Mater. Chem.* **2007**, *17*, 2351–2358.
- [196] H. J. Song, Z. Z. Zhang, X. H. Men, *Eur. Polym. J.* **2008**, *44*, 1012–1022.
- [197] Q. Cheng, V. Pavlinek, Y. He, C. Li, A. Lengalova, P. Saha, *Eur. Polym. J.* **2007**, *43*, 3780–3786.
- [198] X. Zhang, A. J. Du, P. Lee, D. D. Sun, J. O. Leckie, *J. Membr. Sci.* **2008**, *313*, 44–51.
- [199] W. Dong, A. Cogbill, T. Zhang, S. Ghosh, Z. R. Tian, *J. Phys. Chem. B* **2006**, *110*, 16819–16822.
- [200] M. Miyauchi, H. Tokudome, *Appl. Phys. Lett.* **2007**, *91*, 043111–3.
- [201] M. Takahashi, Y. Okada, K. Kobayashi, *Chem. Lett.* **2008**, *37*, 276–277.
- [202] S. M. Moghimi, A. C. Hunter, J. C. Murray, *Pharmacol. Rev.* **2001**, *53*, 283–318.
- [203] W. J. Parak, D. Gerion, T. Pellegrino, D. Zanchet, C. Micheel, S. C. Williams, R. Boudreau, M. A. Le Gros, C. A. Larabell, A. P. Alivisatos, *Nanotechnology* **2003**, *14*, R15–R27.
- [204] D. V. Bavykin, E. V. Milsom, F. Marken, D. H. Kim, D. H. Marsh, D. J. Riley, F. C. Walsh, K. H. El-Abiary, A. A. Lapkin, *Electrochem. Commun.* **2005**, *7*, 1050–1058.
- [205] W. Zheng, Y. F. Zheng, K. W. Jin, N. Wang, *Talanta* **2008**, *74*, 1414–1419.
- [206] A. Liu, M. Wei, I. Honma, H. Zhou, *Anal. Chem.* **2005**, *77*, 8068–8074.
- [207] X. P. Tang, N. C. Ng, H. Nguyen, G. Mogilevsky, Y. Wu, *Chem. Phys. Lett.* **2008**, *452*, 289–295.
- [208] W. Dong, T. Zhang, J. Epstein, L. Cooney, H. Wang, Y. Li, Y. B. Jiang, A. Cogbill, V. Varadan, Z. R. Tian, *Chem. Mater.* **2007**, *19*, 4454–4459.
- [209] S. H. Oh, R. R. Finones, C. Daraio, L. H. Chen, S. Jin, *Biomaterials* **2005**, *26*, 4938–4943.
- [210] Q. Zhou, Y. Ding, J. Xiao, G. Liu, X. Guo, *J. Chromatogr. A* **2007**, *1147*, 10–16.
- [211] X. Ma, T. Zhu, H. Xu, G. Li, J. Zheng, A. Liu, J. Zhang, H. Du, *Anal. Bioanal. Chem.* **2008**, *390*, 1133–1137.
- [212] J. Yin, X. Zhao, *Nanotechnology* **2006**, *17*, 192–196.
- [213] H. Chen, W. Yang, Y. He, Y. Ding, L. Zhang, C. Tan, A. A. Lapkin, D. V. Bavykin, *Powder Technol.* **2008**, *183*, 63–72.

Received: November 18, 2008

Published Online: February 11, 2009